Supernovae in stellar clusters as CR pevatrons

A.M. Bykov
High Energy Astrophysics
Ioffe Institute, St.Petersburg, Russian Federation

Collaborators: D.C.Ellison, P.E.Gladilin, S.M. Osipov

Gamma Ray Spectral Energy Distribution:

Starburst galaxies

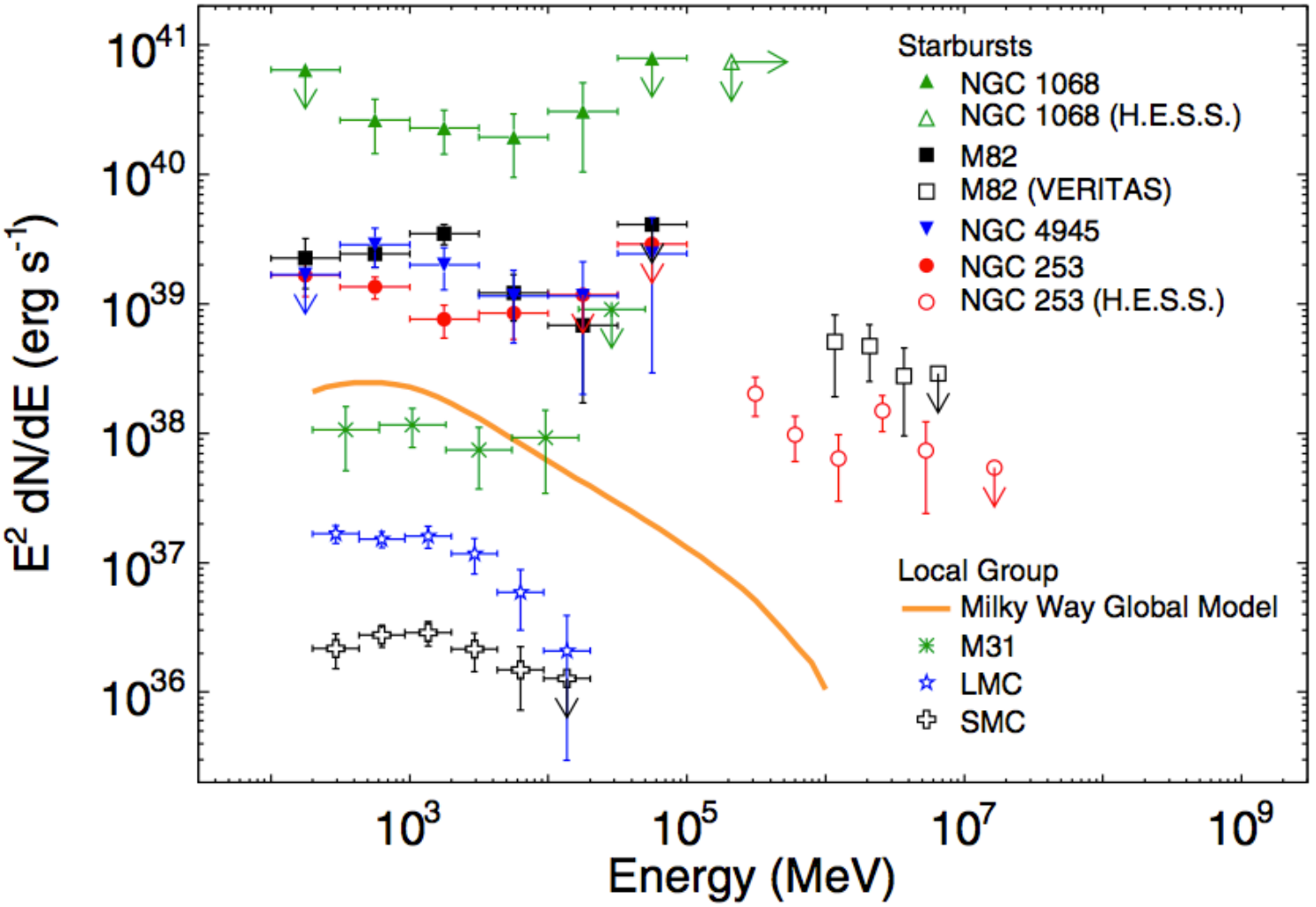

Ackermann + 12

A&ARv v.22, p.54, 2014

S.Ohm, CRePhy, v.17, p. 585, 2016

Gamma Ray Spectral Energy Distribution:

Starburst galaxies

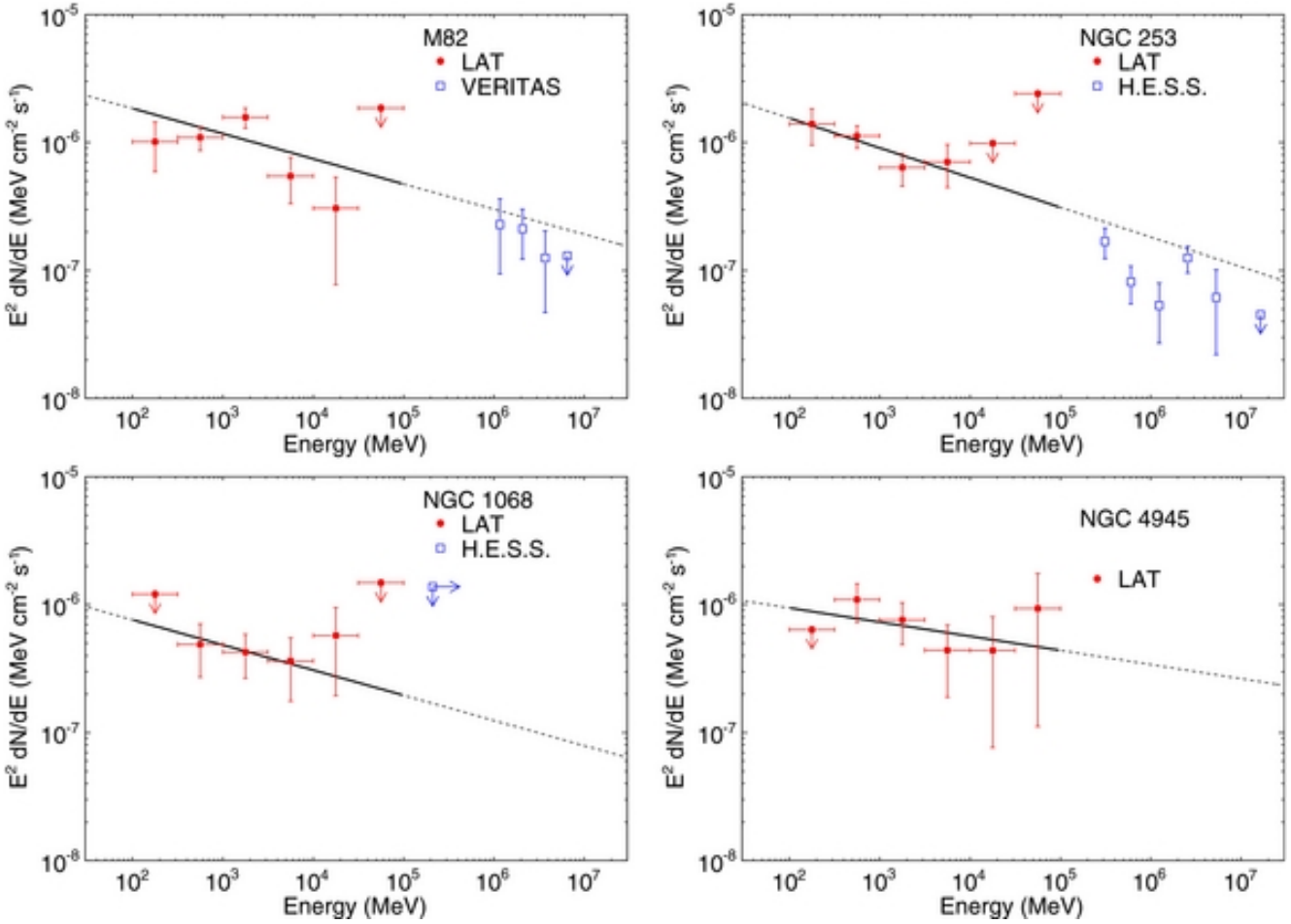

Ackermann + 12

A&ARv v.22, p.54, 2014

S.Ohm, CRePhy, v.17, p. 585, 2016

SFR from FUV+IR

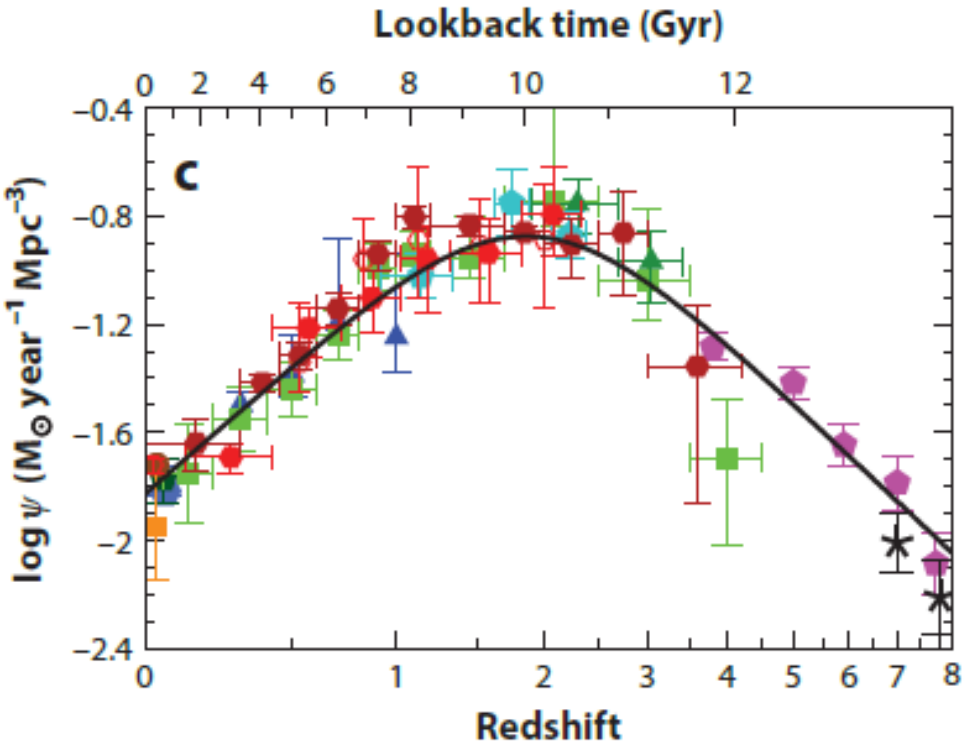

$$\psi(z) = 0.015 \frac{(1+z)^{2.7}}{1+[(1+z)/2.9]^{5.6}} \, \mathrm{M}_\odot \, \mathrm{year}^{-1} \, \mathrm{Mpc}^{-3}.$$

Madau & Dickinson, ARAA 2014

Core-collapse - SN rate

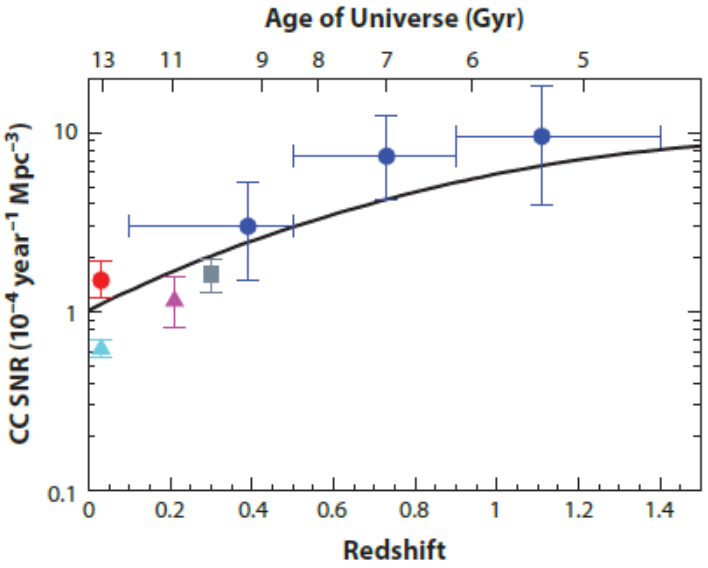

Figure 10

The cosmic core-collapse supernova (SN) rate. The data points are taken from Li et al. (2011) (*cyan triangle*), Mattila et al. (2012) (*red dot*), Botticella et al. (2008) (*magenta triangle*), Bazin et al. (2009) (*gray square*), and Dahlen et al. (2012) (*blue dots*). The solid line shows the rates predicted from our fit to the cosmic star-formation history. The local overdensity in star formation may boost the local rate within 10–15 Mpc of Mattila et al. (2012).

$$R_{\rm CC}(z) = \psi(z) \times \frac{\int_{m_{\rm min}}^{m_{\rm max}} \phi(m){\rm d}m}{\int_{m_l}^{m_u} m\phi(m){\rm d}m} \equiv \psi(z) \times k_{\rm CC}, \qquad (16)$$

where the number of stars that explode as SNe per unit mass is $k_{\rm CC} = 0.0068\ {\rm M}_\odot^{-1}$ for a Salpeter IMF, $m_{\rm min} = 8\,{\rm M}_\odot$ and $m_{\rm max} = 40\,{\rm M}_\odot$. The predicted cosmic SN rate is shown in **Figure 10**

Madau & Dickinson, ARAA 2014

Cluster formation efficiency

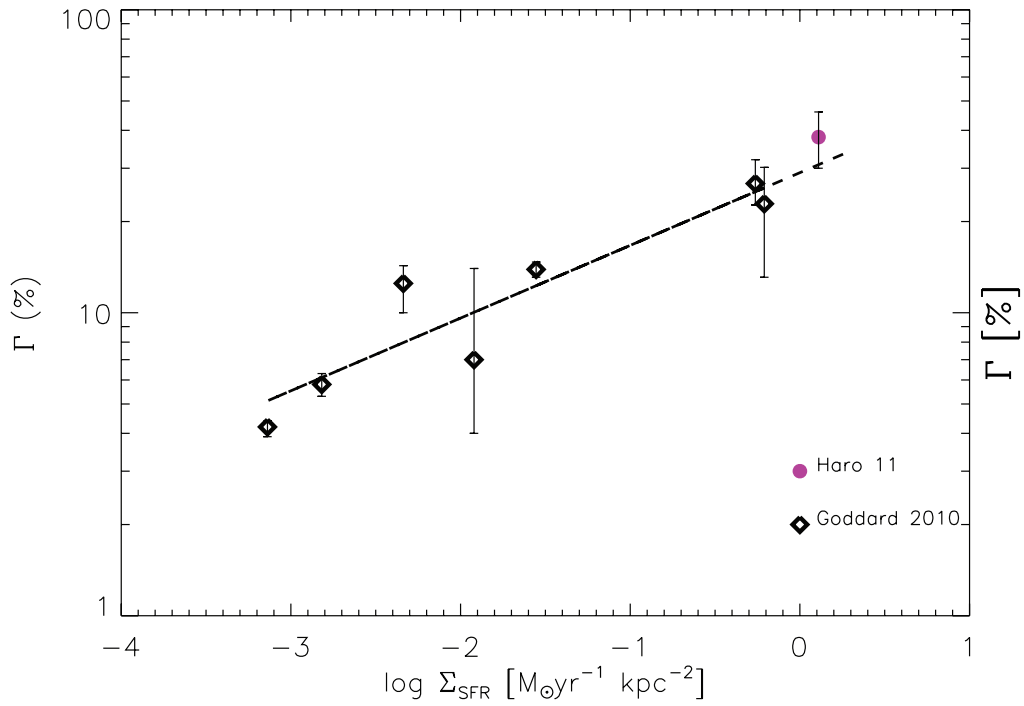

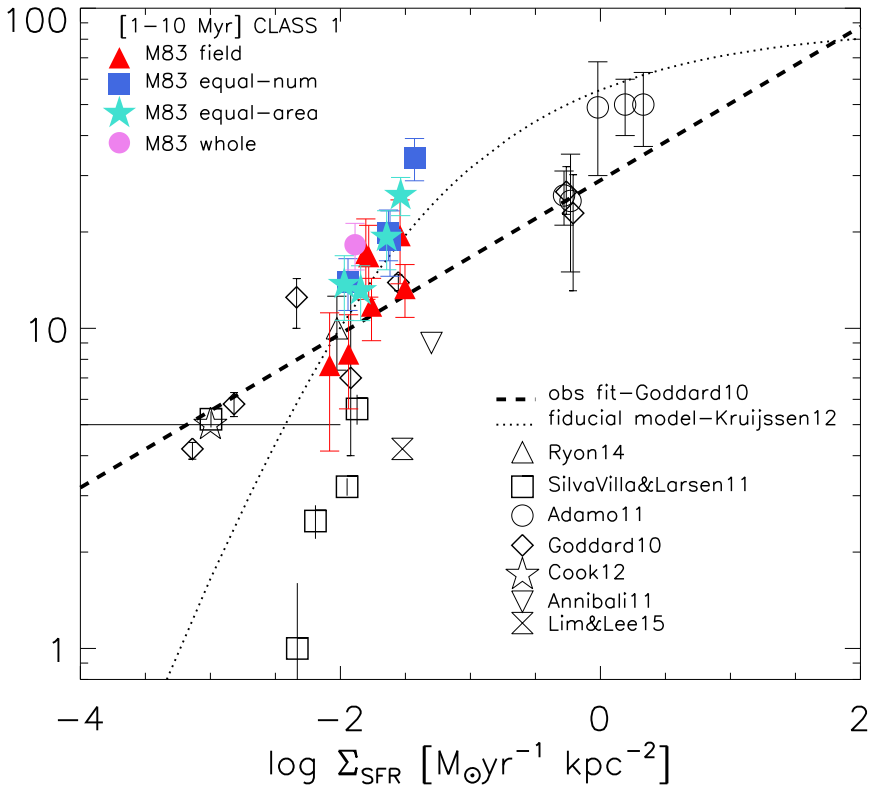

Figure 23. Cluster formation efficiency, Γ, as a function of the galactic SFR density, Σ_{SFR}. The black diamonds are the galaxy sample of Goddard et al. (2010) which were used to obtain the best-fitting power-low relation shown by the dashed line (Goddard et al. 2010, their equation 3). At the right-hand end we show the position of Haro 11 (filled dots) which fits the relation nicely despite its extreme Γ and SFR values.

SFR in Haro 11 galaxy is about 22 Msun/yr

Adamo + 2010

Adamo & Bastian 2016

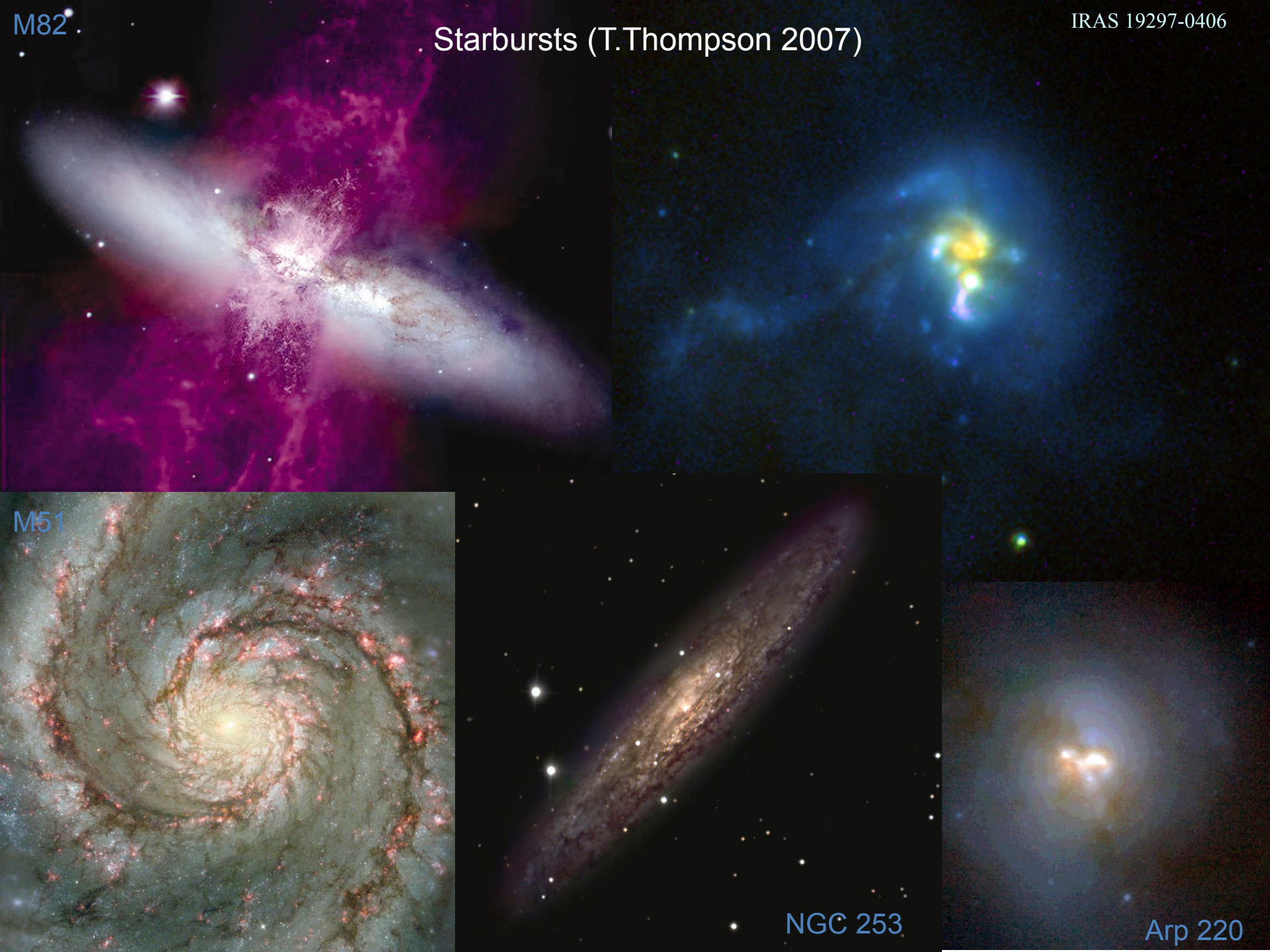
M82
Starbursts (T.Thompson 2007)
IRAS 19297-0406
M51
NGC 253
Arp 220

Nearest Merger—The “Antennae”

- WFPC2, with CO overlay (Whitmore et al. 1999; Wilson et al. 2000)
- VLA 5 GHz image (Neff & Ulvestad 2000)

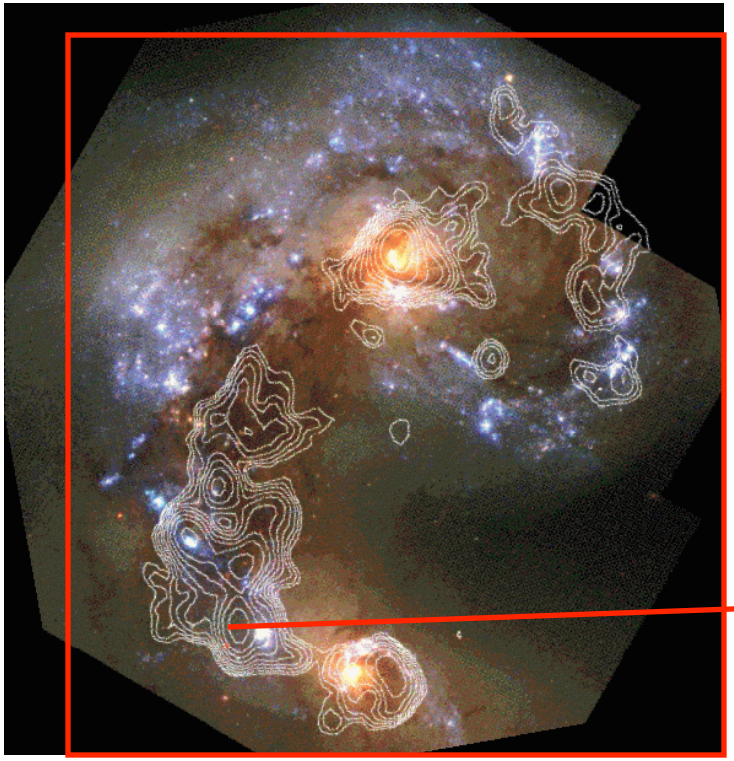

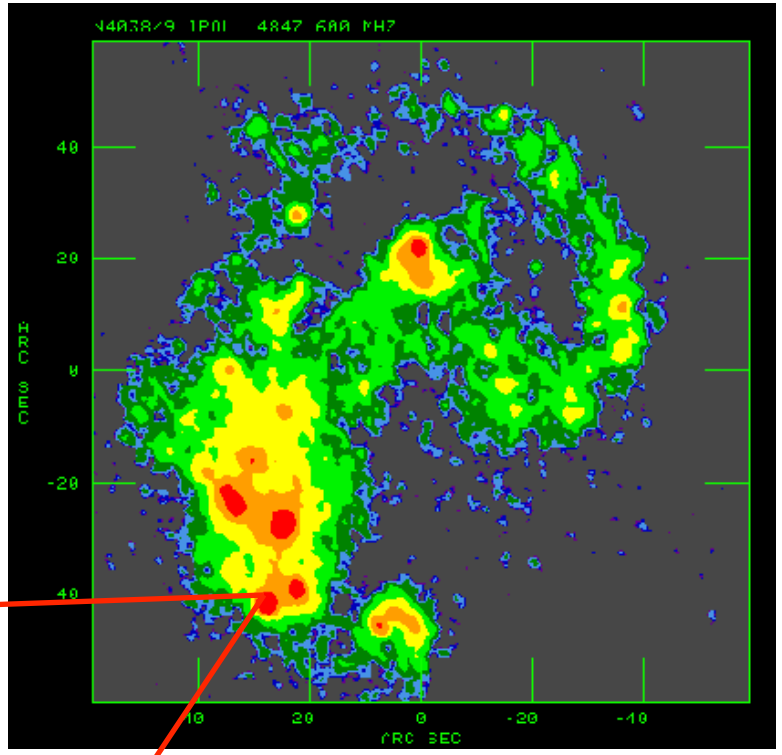

5 mJy ≈ 30,000 O7-equivalent stars

Magnetic Fields in starbursts from radio observations

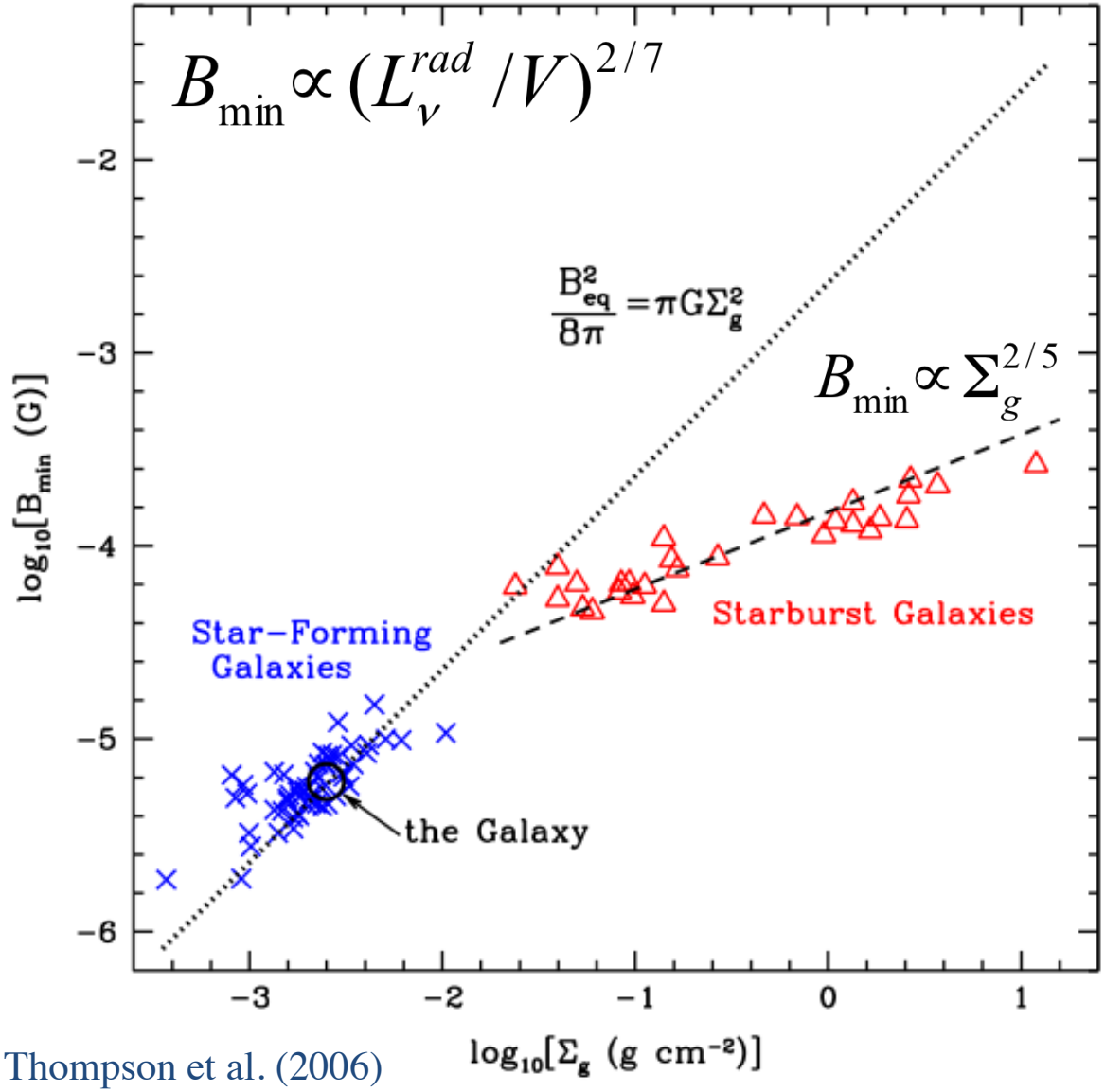

Thompson et al. (2006)

If a fraction ~1% of 10^{51} ergs per SN goes to CR electrons, **and they cool rapidly**, the observed trend is reproduced.

What are the HECR sources in starforming / starburst regions?

SNR in Molecular Clouds

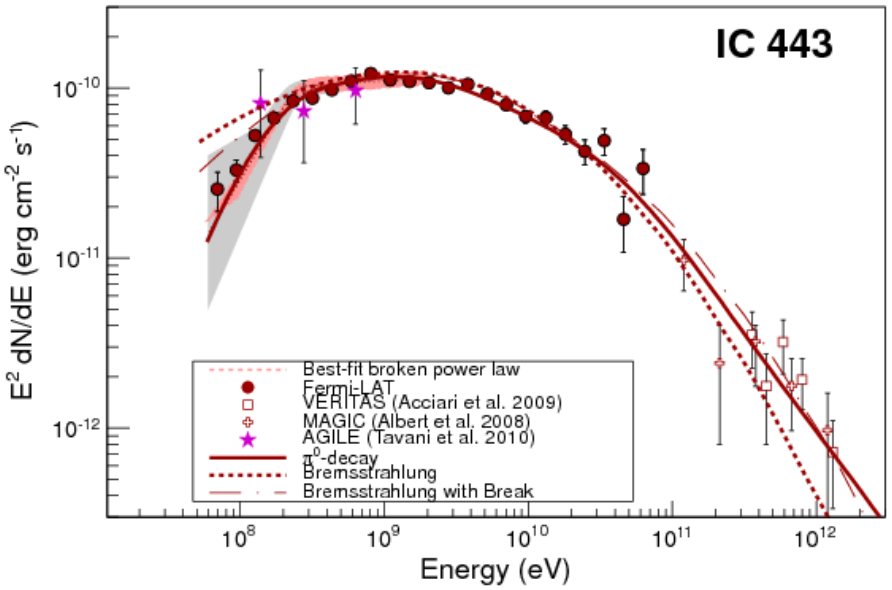

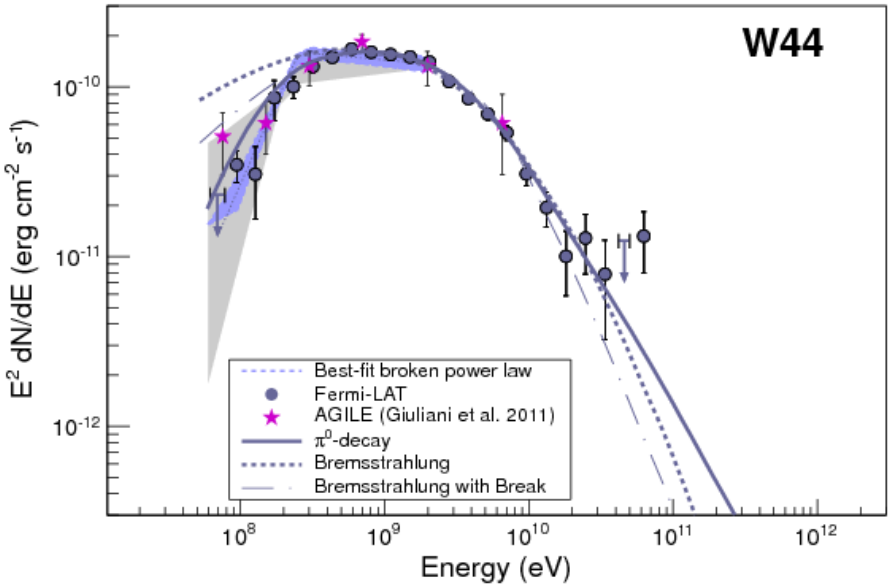

M.Ackermann 2013

Pion-Decay Signatures

see: Tavani + 2010, Uchiyama+ 2010, Giuliani+ 2011, Ackermann+ 2013, Cardillo+ 2014

Observed gamma-ray spectra of SNRs

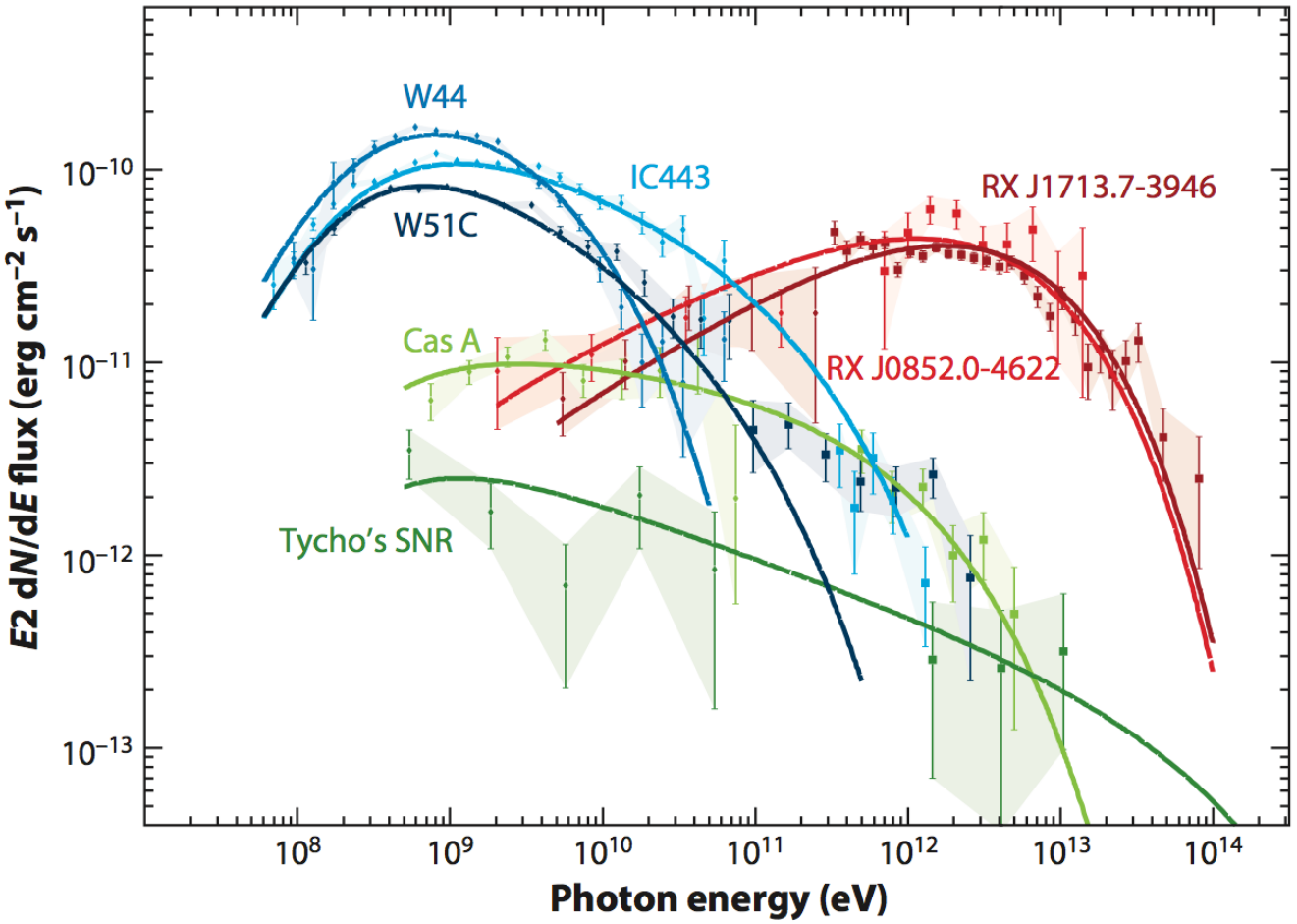

S. Funk 2015

- ***What are the sources of PeV regime CRs?***

PeV CRs are likely accelerated in the Galaxy

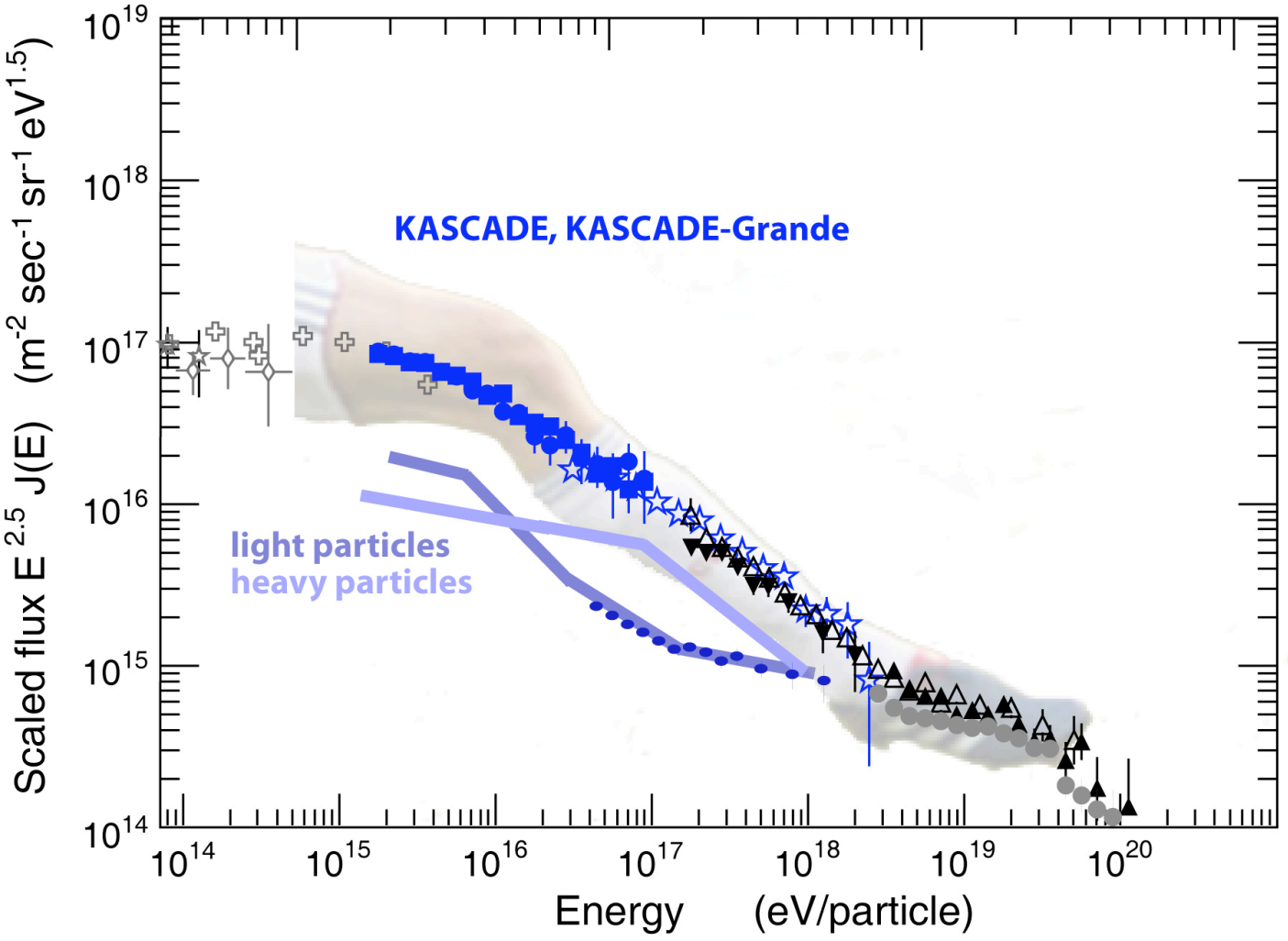

How to get PeV energy CRs?

Rare SNe with a special CSM type IIn?

Rare magnetar-driven SNe?

Clustered YMS-SNRs (superbubbles)?

SNR- Stellar/Custer Wind collision?

- **From a general constraint on the CR acceleration rate the "luminosity" of NR MHD flow should exceed:**

$$L_{\rm tot} > 6 \times 10^{40}\, Z^{-2} \beta_{\rm sh}^{-1}\, \Theta^2\, \mathcal{E}_{P8}\ {\rm erg\,s^{-1}}$$

$$\text{for a SN in SSC (age}\, 400\, \text{yrs)}$$

$$L_{\rm kin} \leq 10^{41}\ {\rm erg\,s^{-1}}$$

cf F.Aharonian, M.Lemoine, E.Waxman …

PeV proton acceleration in young SNe

CR proton acceleration by radio SNe and trans-relativistic SNRs

V. Tatischeff: Radio emission and nonlinear diffusive shock acceleration in SN 1993J

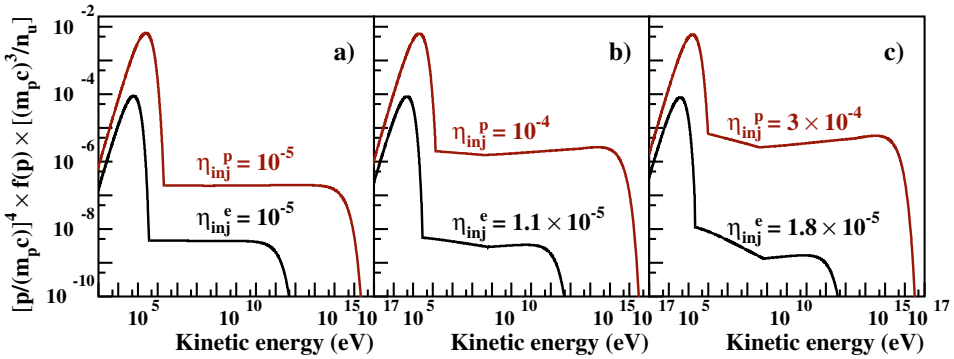

V.Tatischeff 2009

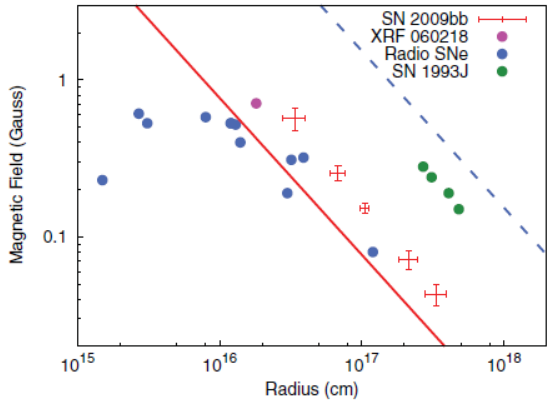

Figure 1. Hillas Diagram: Mildly relativistic sources ($\beta/\Gamma \sim 1$) must lie above the *solid line*, to accelerate Iron nuclei to 60 EeV by diffusive shock acceleration, according to $E_Z \lesssim \beta e Z B R/\Gamma$. Non-relativistic SNe ($\beta/\Gamma \sim 0.05$) must lie above the *dashed line* to reach the same energies. Radius and magnetic field of SN 2009bb (crosses, at 5 epochs, determined here from radio observations with VLA and GMRT assuming equipartition) and XRF 060218 lie above the solid red line. Other balls denote other radio SNe from Chevalier (1998). For SN 1993J only, the magnetic fields are obtained by Chandra, Ray, & Bhatnagar (2004) without assuming equipartition. All non-relativistic SNe including SN 1993J lie below the dashed line and are unable to produce UHECRs unlike the mildly relativistic SN 2009bb and XRF 060218 which lie above the solid line.

S.Chakraborti, A.Ray, A.Soderberg, A.Loeb, P.Chandra 2011

Rare types of SNe

CR proton acceleration by SNe type IIn with dense pre-SN wind

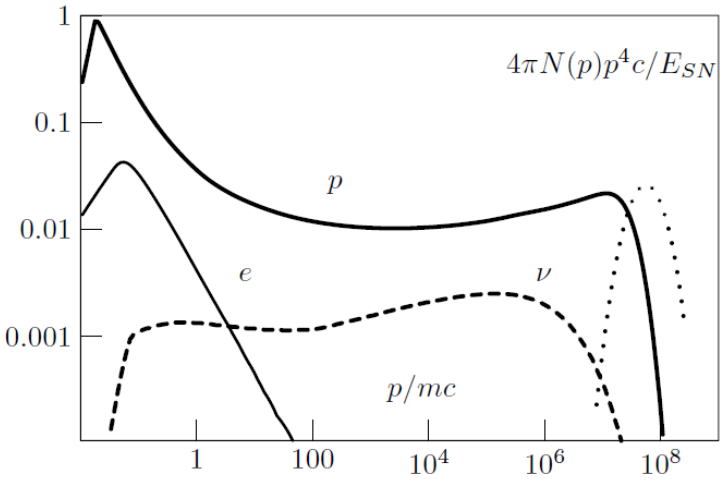

Figure 4: Spectra of particles produced in the supernova remnant during 30 yr after explosion. The spectrum of protons (thick solid line), the spectrum of secondary electrons (multiplied on 10^3, thin solid line), the spectrum of neutrinos (thick dashed line) are shown.

CR proton acceleration by Type IIn SNe
V. Zirakashvili & V. Ptuskin 2015

CR proton acceleration in trans-relativistic SNe Ibc
SNe Ibc occur mostly in gas-rich star-forming spirals

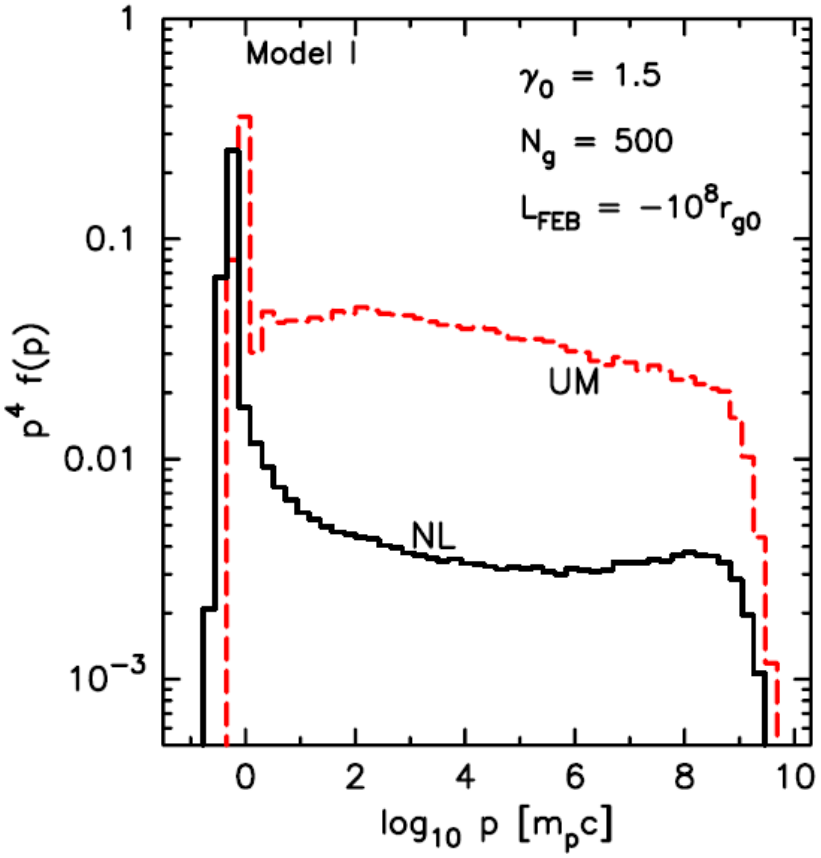

CR proton acceleration by trans-relativistic SNe $\beta/\Gamma \sim 1$
Ellison, Warren, Bykov
ApJ v.776, 46, 2013

What else one could expect in starburst?
Superbubble caverns with multiple shocks.

Hadronic gamma-ray emission from superbubbles?

Fermi image of Cygnus superbubble

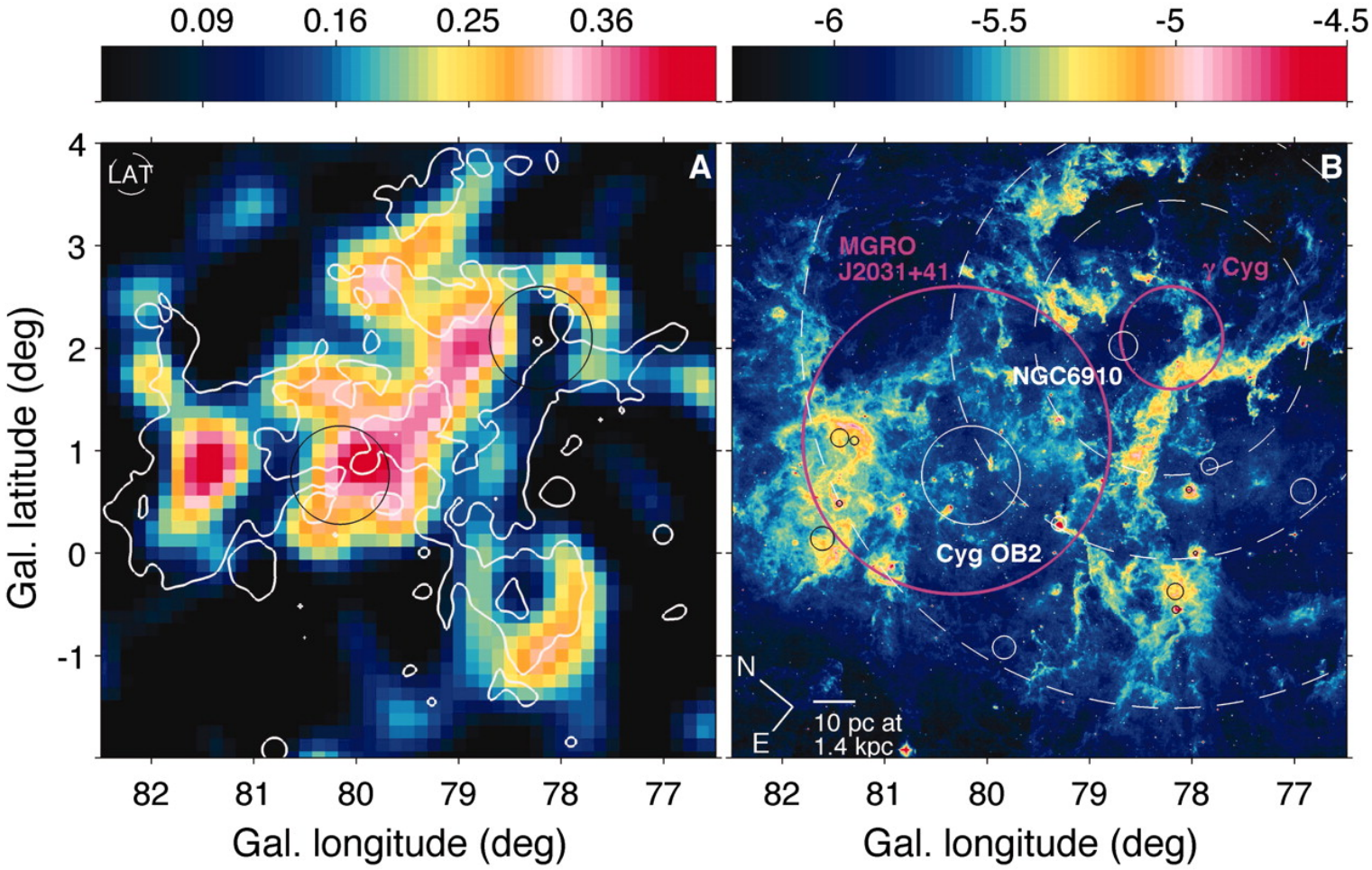

Ackermann + 2011

Fermi spectrum of Cygnus superbubble

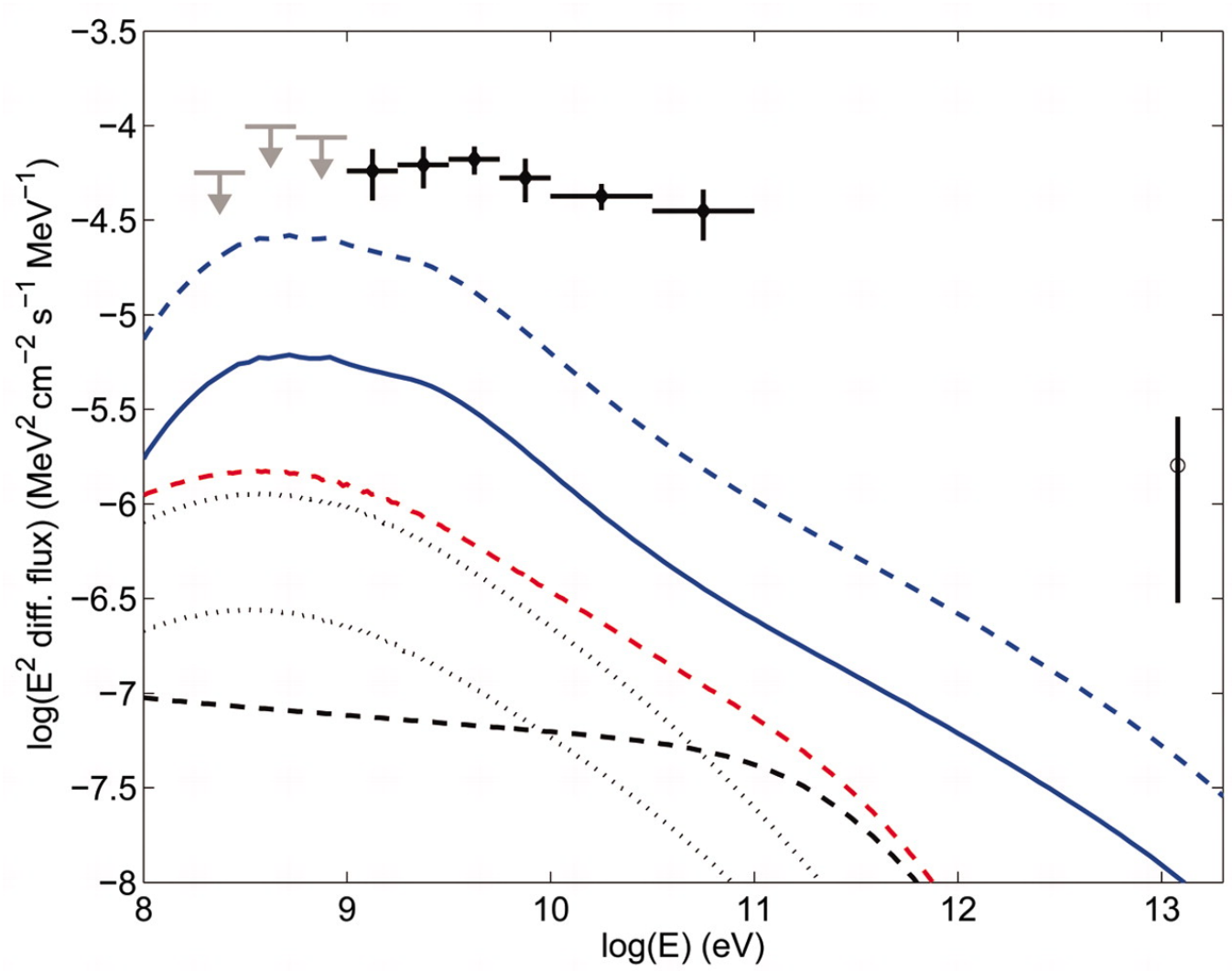

Ackermann + 2011

The Fermi source is extended of about 50 pc scale size and anti-correlate with MSX

Cygnus X is about 1.5 kpc away. Contain a number of young star clusters and several OB associations. Cygnus OB2 association contains 65 O stars and more than 500 B stars. There is a young supernova remnant Gamma-Cygni and a few gamma-pulsars.

PeV proton acceleration by SNe in young compact stellar clusters & starbursts

SNR - cluster wind accelerator

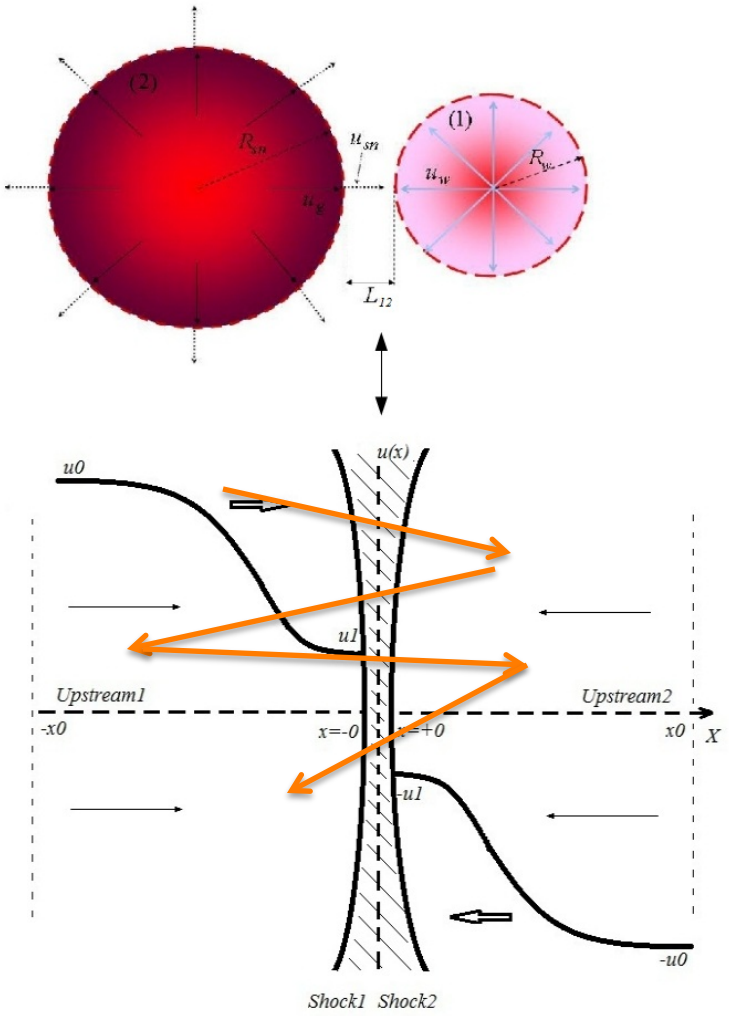

MNRAS V. 429, 2755, 2013

Colliding shock flow geometry used
Shock was divided in a few sections

Stellar wind shock
(thin shell approximation)
Wilkin 1996

$$R(\theta) = \sqrt{\frac{\dot{m}V_w}{4\pi\rho_a V_*^2}} \cdot \frac{\sqrt{3(1-\theta ctg\theta)}}{sin\theta}$$

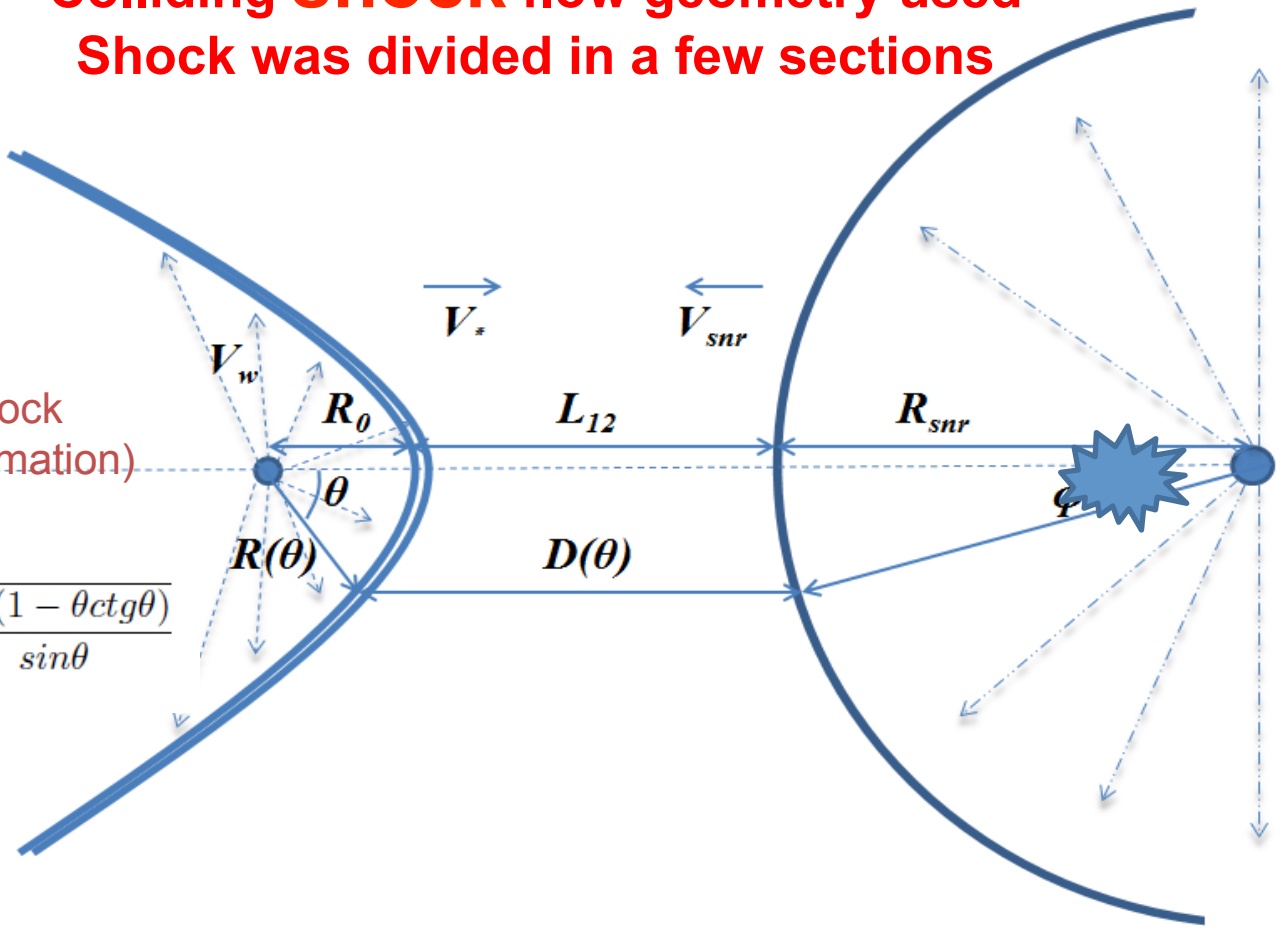

SNR-stellar wind accelerator
Non-linear kinetic model

Transport equation for CR distribution function

$$u(x)\frac{\partial f(x,p)}{\partial x} - \frac{\partial}{\partial x}\left[D(x,p)\frac{\partial}{\partial x}f(x,p)\right] =$$

$$= \frac{p}{3}\frac{du(x)}{dx}\frac{\partial f(x,p)}{\partial p} + Q(x,p)\delta(x). \qquad (1)$$

The momentum conservation equation, normalized to $\rho_0 u_0^2$ reads

$$U(x) + P_c(x) + P_w(x) + P_g(x) = 1 + \frac{1}{\gamma M_0^2}\,,$$

where M_0 is the Mach number of the unperturbed flow. The normalized cosmic ray pressure

$$P_c(x) = \frac{4\pi}{3\rho_0 u_0^2}\int_{p_{inj}}^{\infty} dp\; p^3\; v(p)\; f(x,p)\,, \qquad (2)$$

MNRAS V. 429, 2755, 2013

SNR-stellar wind accelerator

$$f(x,p) = f_0 \exp\left[-\int_x^0 dx' \frac{u(x')}{D(x',p)}\right]\left[1 - \frac{W(x,p)}{W_0(p)}\right], \quad (1)$$

$$\phi_{esc}(p) = -\frac{u_0 f_0}{W_0(p)} \quad (2)$$

where $D(x,p)$ is the CR diffusion coefficient,

$$W(x,p) = u_0 \int_x^0 dx' \frac{\exp\left[-\psi(x',p)\right]}{D(x',p)}, \quad (3)$$

$$\psi(x,p) = -\int_x^0 dx' \frac{u(x')}{D(x',p)}, \quad (4)$$

and $W_0(p) = W(x_0,p)$.

cf Malkov' 97; Amato & Blasi 05; Caprioli + 11

MNRAS V. 429, 2755, 2013

SNR-stellar wind accelerator

We solve one-dimensional transport equations for the pitch-angle-averaged phase space distribution function of protons, $f_p(x,p,t)$, and electrons, $f_e(x,p,t)$, given by

$$\tau(p)\frac{\partial^2 g_p}{\partial t^2}+\frac{\partial g_p}{\partial t}+u(x)\frac{\partial g_p}{\partial x}-\frac{1}{3}\frac{\partial u(x)}{\partial x}\left(\frac{\partial g_p}{\partial y}-4g_p\right)= \frac{\partial}{\partial x}\left(D(x,p)\frac{\partial g_p}{\partial x}\right), \quad (1)$$

$$\tau(p)\frac{\partial^2 g_e}{\partial t^2}+\frac{\partial g_e}{\partial t}+u(x)\frac{\partial g_e}{\partial x}-\frac{1}{3}\frac{\partial u(x)}{\partial x}\left(\frac{\partial g_e}{\partial y}-4g_e\right)= \frac{\partial}{\partial x}\left(D(x,p)\frac{\partial g_e}{\partial x}\right)+\exp(y)\frac{\partial}{\partial y}\left[b\exp(-2y)g_e\right], \quad (2)$$

where $g_p = p^4 f_p$, $g_e = p^4 f_e$, $y = ln(p)$.

MNRAS v. 429, 2755, 2013

SNR-stellar wind accelerator

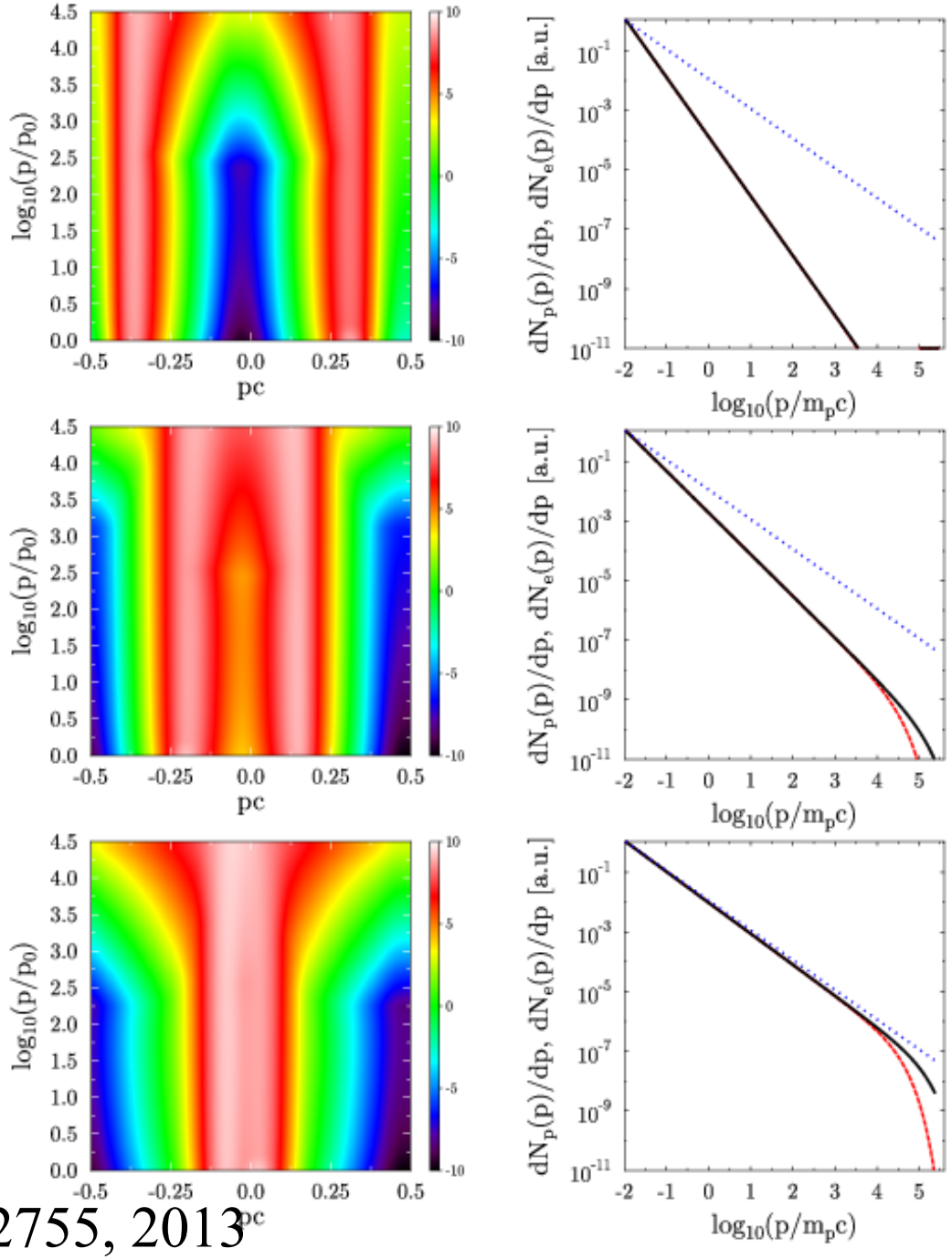

AB+ MNRAS v. 429, 2755, 2013

Particle acceleration between approaching shocks is the most efficient version of Fermi I acceleration

Particle acceleration in colliding shocks is the most plausible scenario for SNe in young compact stellar clusters & starbursts

Acceleration time in the test particle approximation for Bohm diffusion

$$\tau_a \approx \frac{cR_g(p)}{u_s\, u_w}.$$

Acceleration time is about 500 yrs for 10-40 PeV

$$\tau_a \approx 2 \cdot 10^{10}\, \mathcal{E}_{\rm PeV}\, (\eta_b n)^{-0.5}\, u_{s3}^{-2}\, u_{w3}^{-1}\ ({\rm s})$$

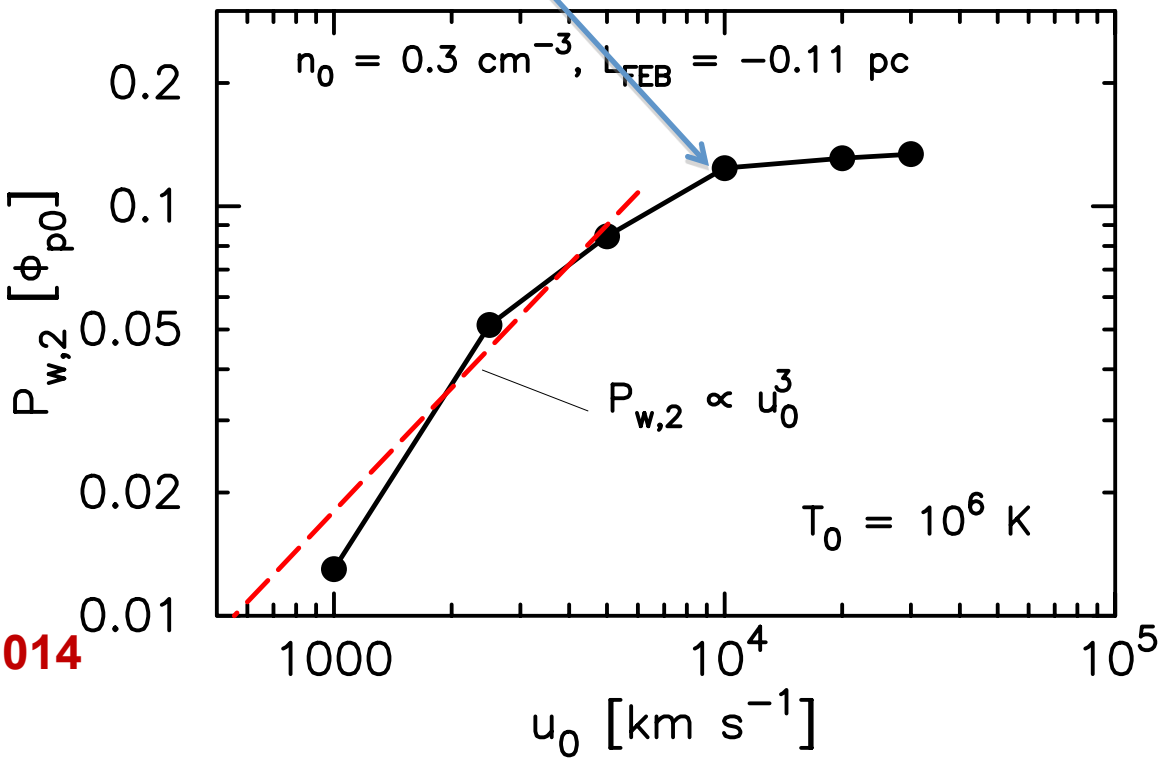

Magnetic field amplification by CR current driven instabilities: Bell's and LW

ApJ v.789, 137, 2014

MAGNETAR-POWERED SUPERNOVAE IN TWO DIMENSIONS. SUPERLUMINOUS SUPERNOVAE

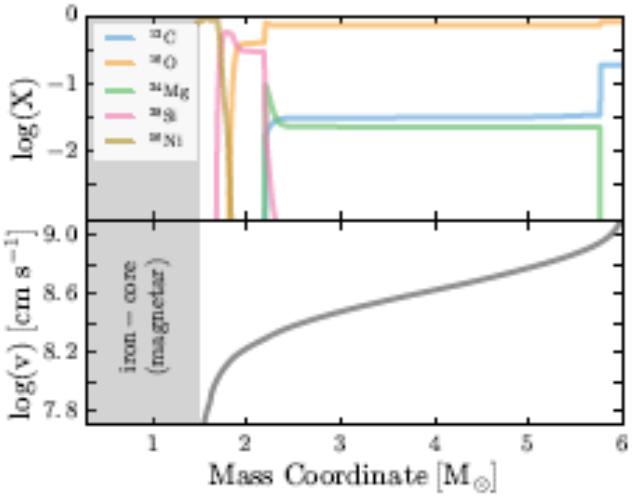

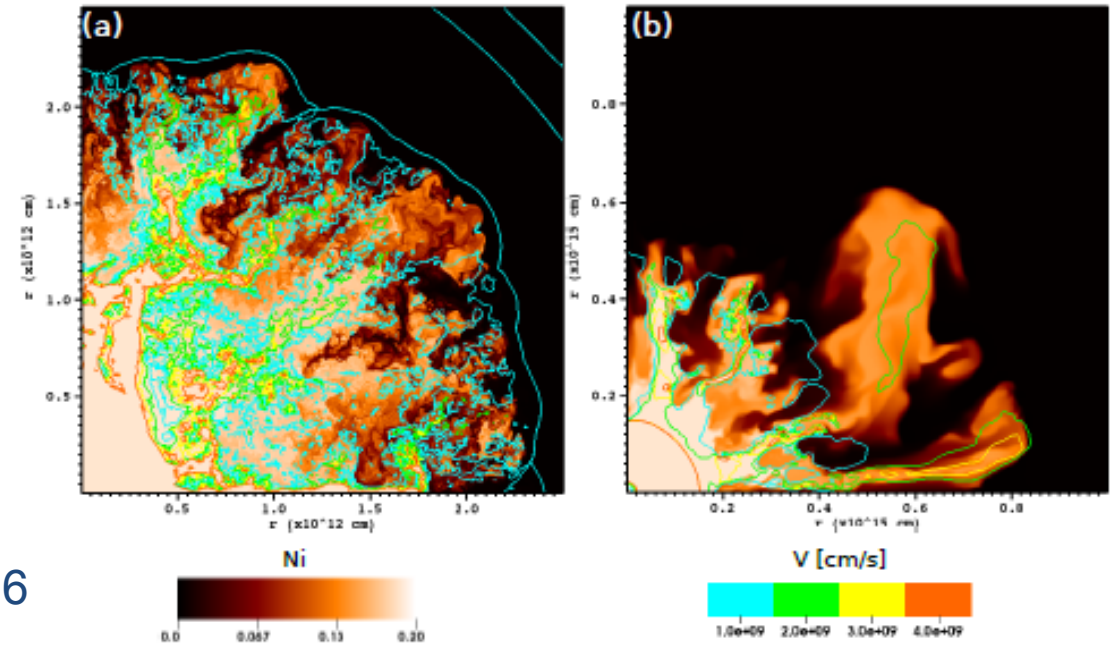

Chen, Woosley & Sukhbold 2016

FIG. 12.— 2D ^{56}Ni and velocity distributions for the 1 ms model (Panel a) and 5 ms model (Panel b) at the last model calculated. ^{56}Ni is mixed out with velocities of 1×10^9 cm s^{-1}. In Panel a, the entire shell has reached the weak breakout regime and will become optically thin region when the strong breakout occurs. In Panel b, two prominent ^{56}Ni fingers appear at the breakout phase. The mixing of ^{56}Ni and other chemical elements may be reflected in the spectrum.

SNe in COMPACT CLUSTER of YOUNG MASSIVE STARS

$$L_\gamma \approx 10^{34} \left(\frac{\eta_p}{0.1}\right) \left(\frac{L_{\rm kin}}{10^{39}{\rm erg\,s^{-1}}}\right) \left(\frac{n}{\rm cm^{-3}}\right) \left(\frac{\tau_a}{5\times 10^{10}\,{\rm s}}\right) {\rm erg\,s^{-1}},$$

@ GC or starbursts $\mathrm{n} \sim 100\,\mathrm{cm}^{-3}$, $L_\gamma \sim 10^{36}\,\mathrm{erg\,s}^{-1}$

A Galactic Super Star Cluster

2MASS Atlas Image from M.Muno

- Distance: 5kpc
- Mass: 10^5 M_{sun}
- Core radius: 0.6 pc
- Extent: ~6 pc across
- Core density:~10^6 pc^{-3}
- Age: 4 +/- 1 Myr
- Supernova rate: 1 every 10,000 years

Chandra Observations

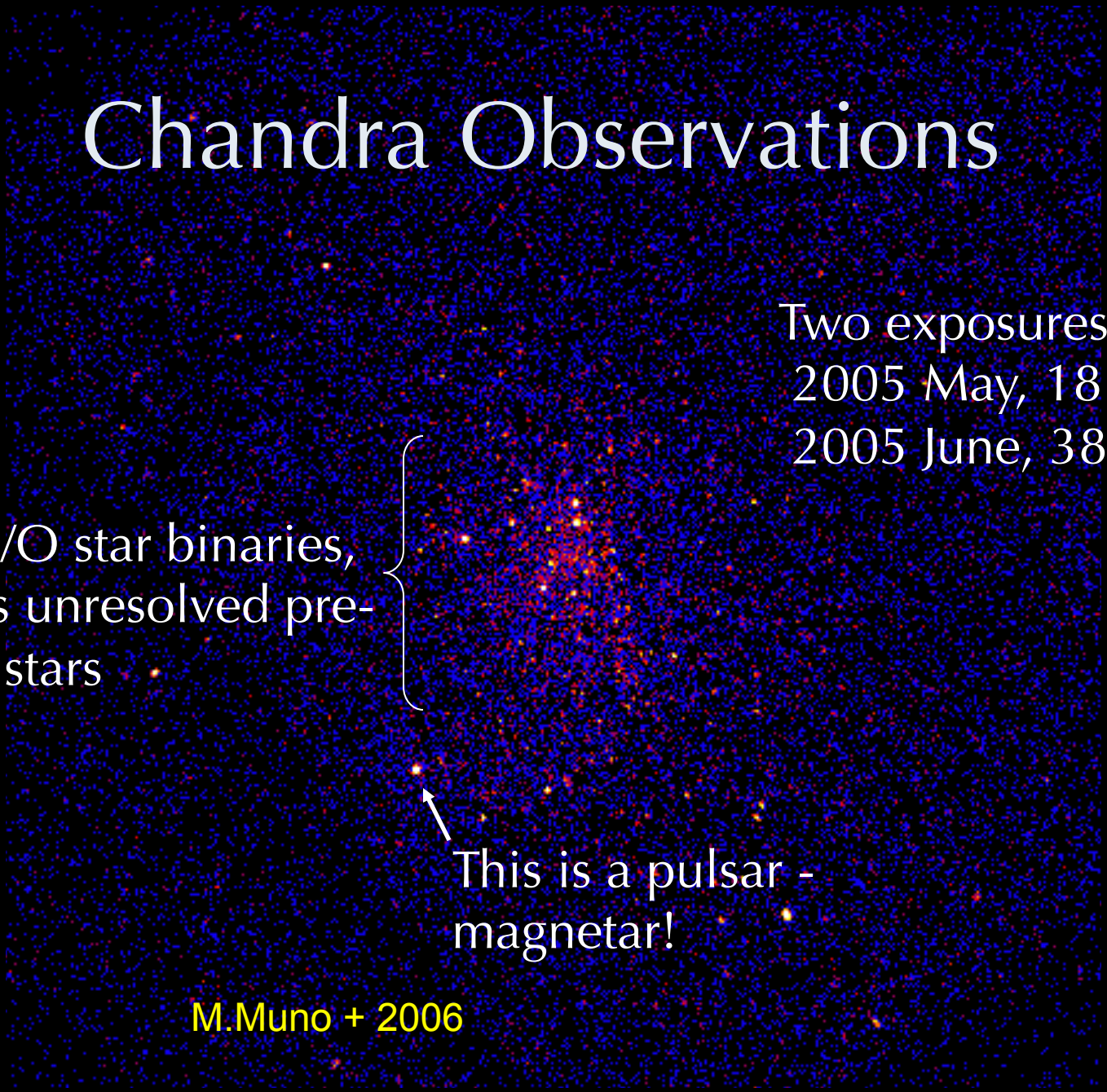

Westerlund 1

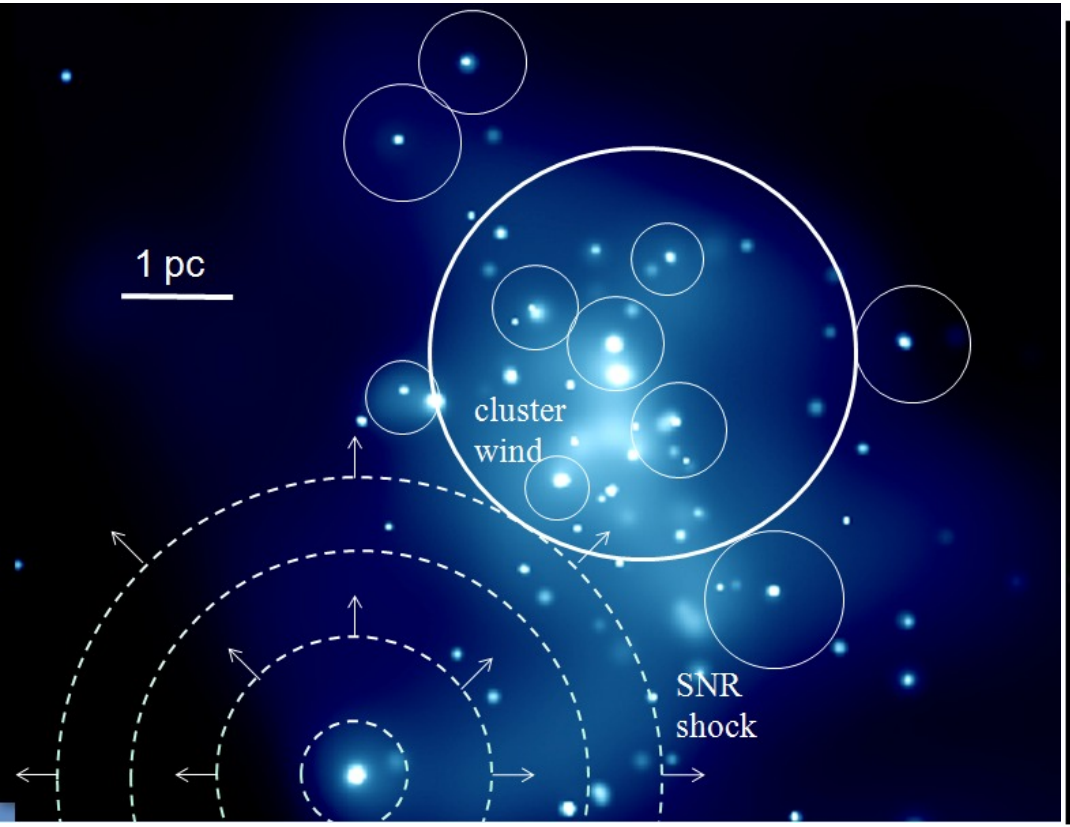

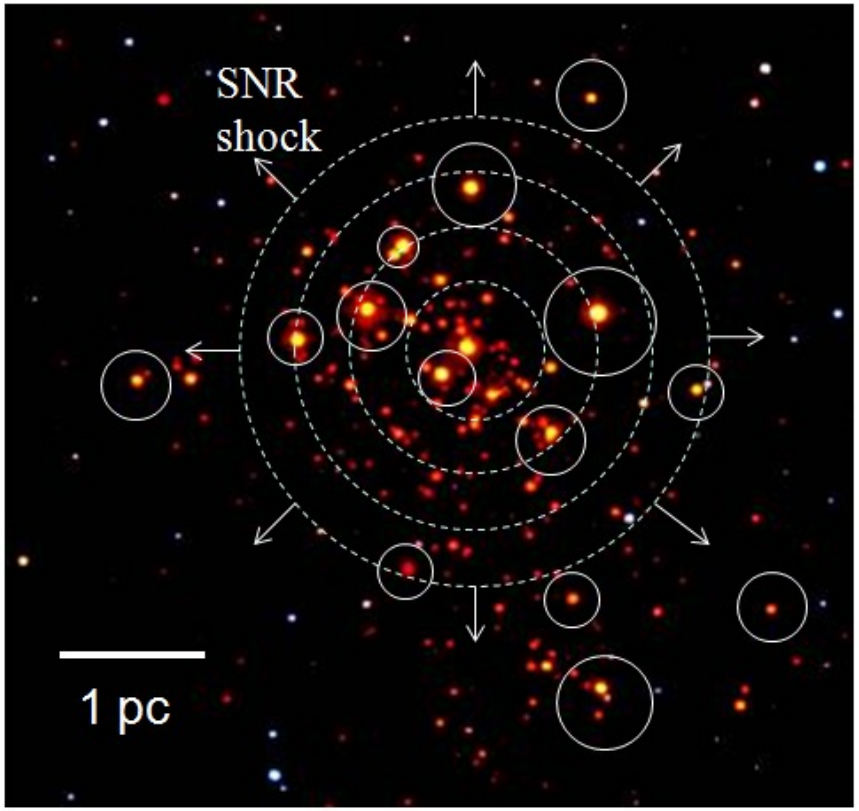

Muno+ 05

Clark+ 05

H.E.S.S. image of Westerlund I

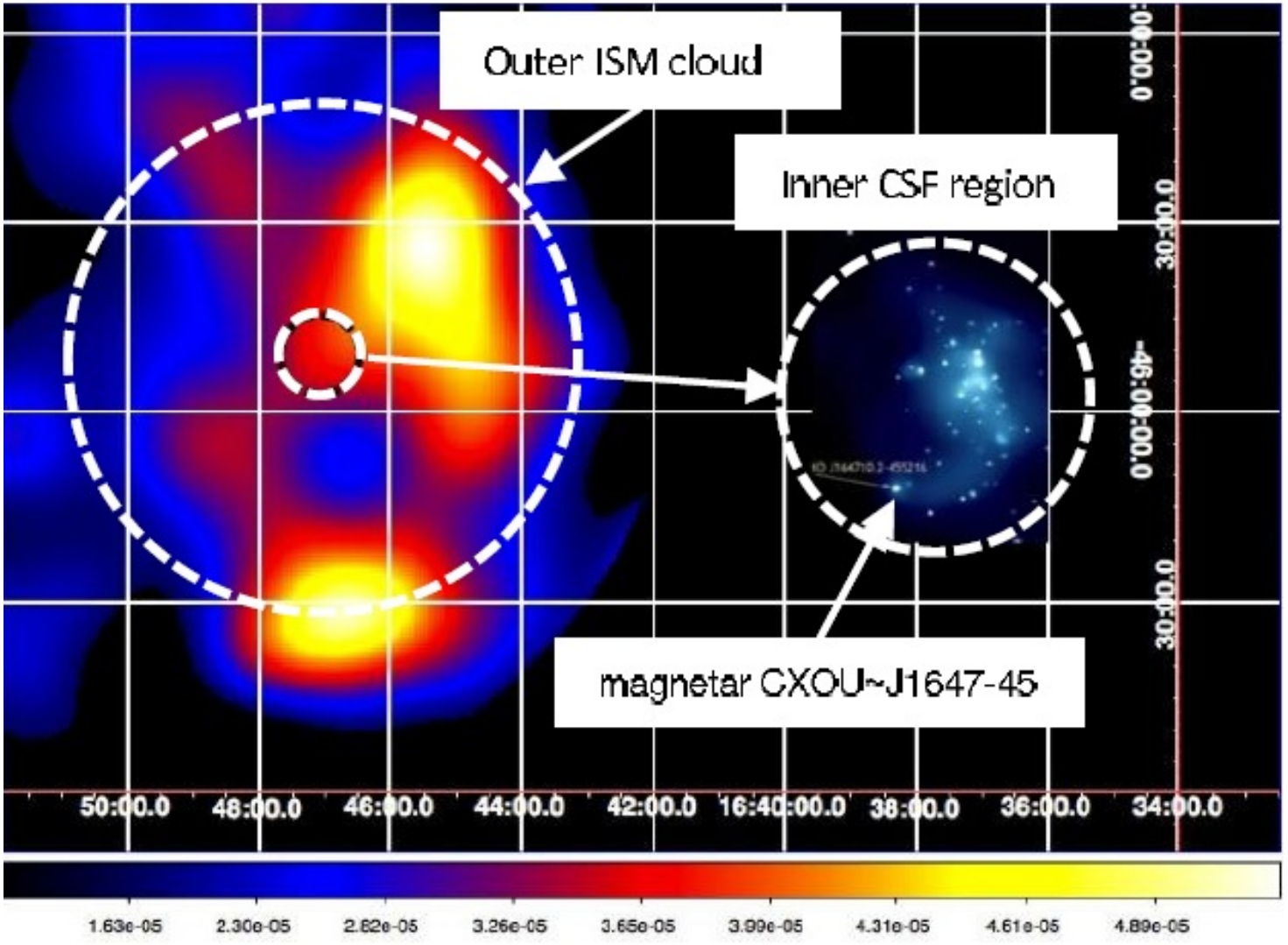

MNRAS v. 453, p. 113, 2015

Gamma Rays and Neutrinos

gamma-rays and high-energy neutrinos :

$$pp, p\gamma \rightarrow \pi^{+} \rightarrow \mu^{+} + \nu_{\mu}$$
$$\rightarrow e^{+} + \nu_{e} + \bar{\nu}_{\mu}$$
$$\rightarrow \pi^{-} \rightarrow \mu^{-} + \bar{\nu}_{\mu}$$
$$\rightarrow e^{-} + \bar{\nu}_{e} + \nu_{\mu}$$

$$\rightarrow \pi^{0} \rightarrow \gamma\gamma$$

gamma rays

we also get γ's from electrons (NB, inverse Compton)

Gamma-rays from a Pevatron

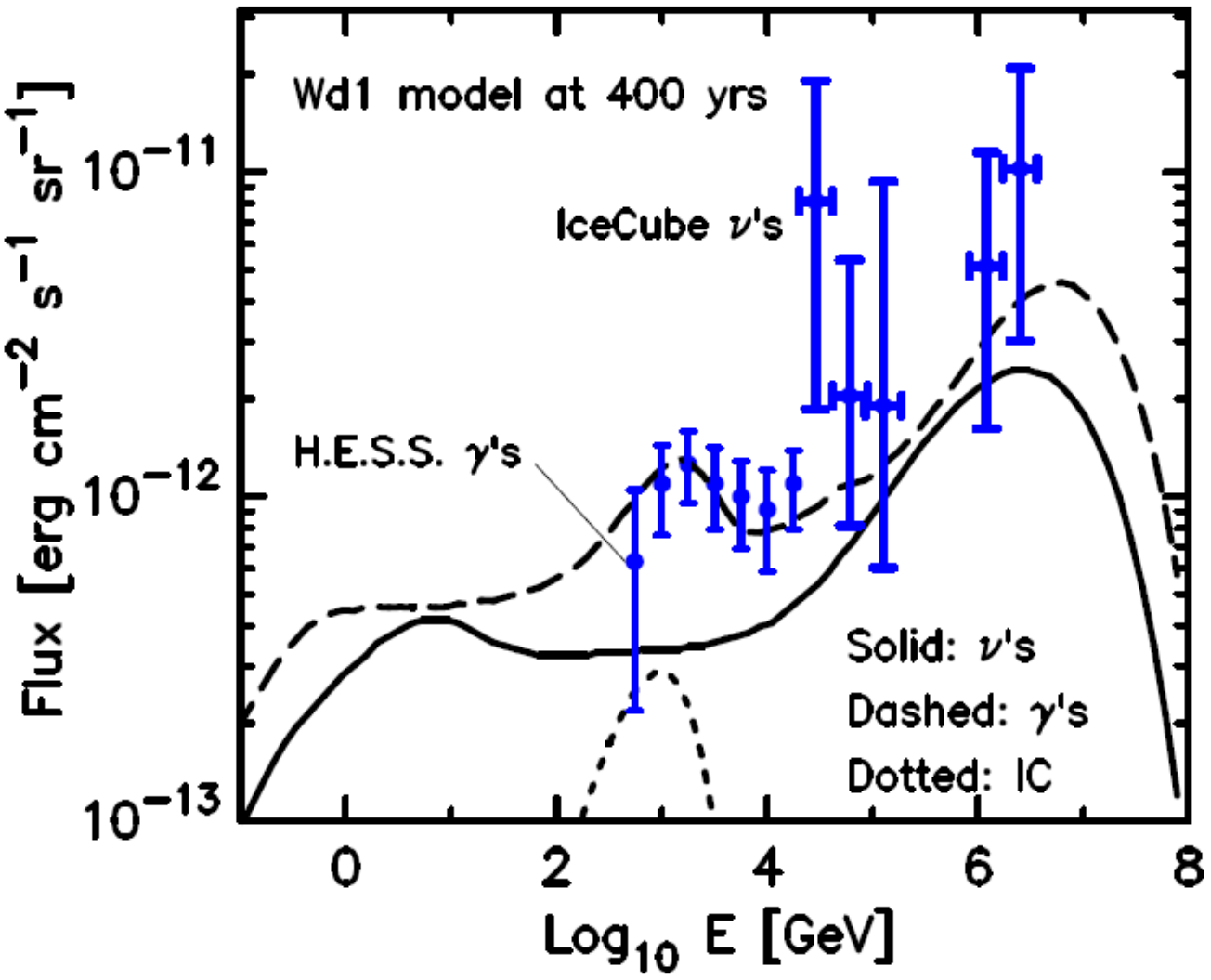

AARv v.22, p.54, 2014
MNRAS V. 453, p. 113, 2015

Gamma-rays from a Pevatron

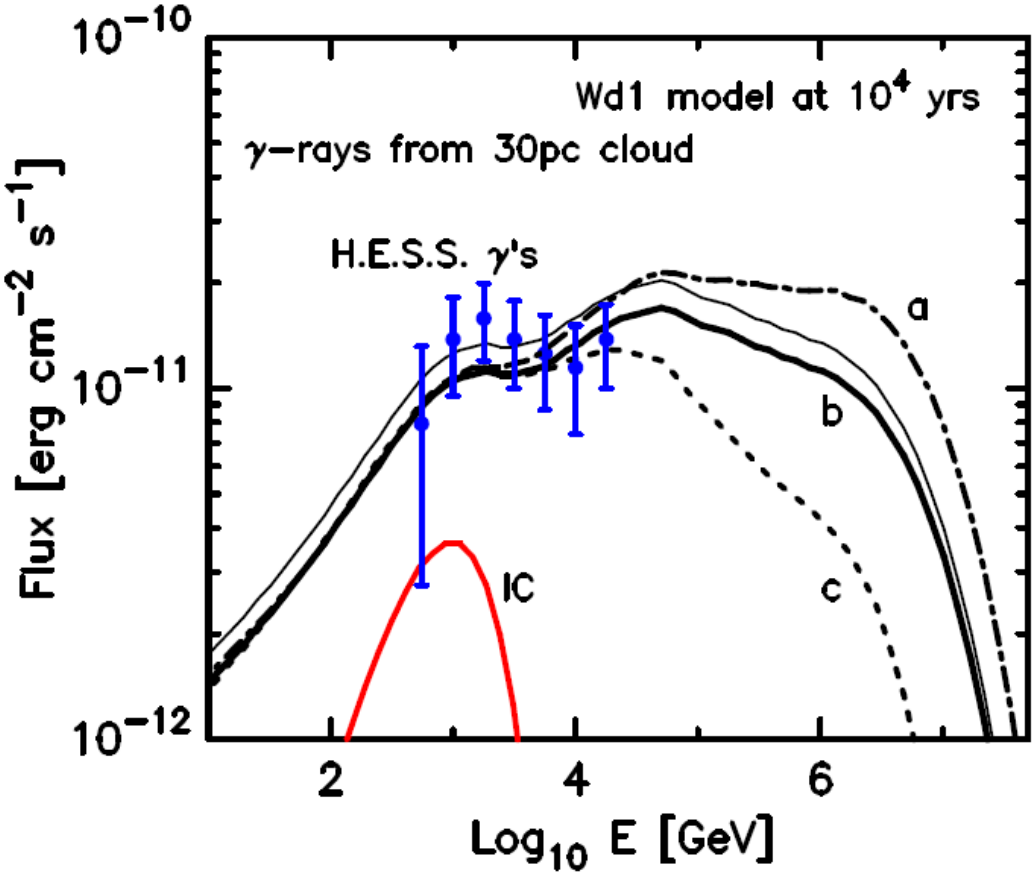

MNRAS V. 453, p. 113, 2015

Neutrinos from a Pevatron

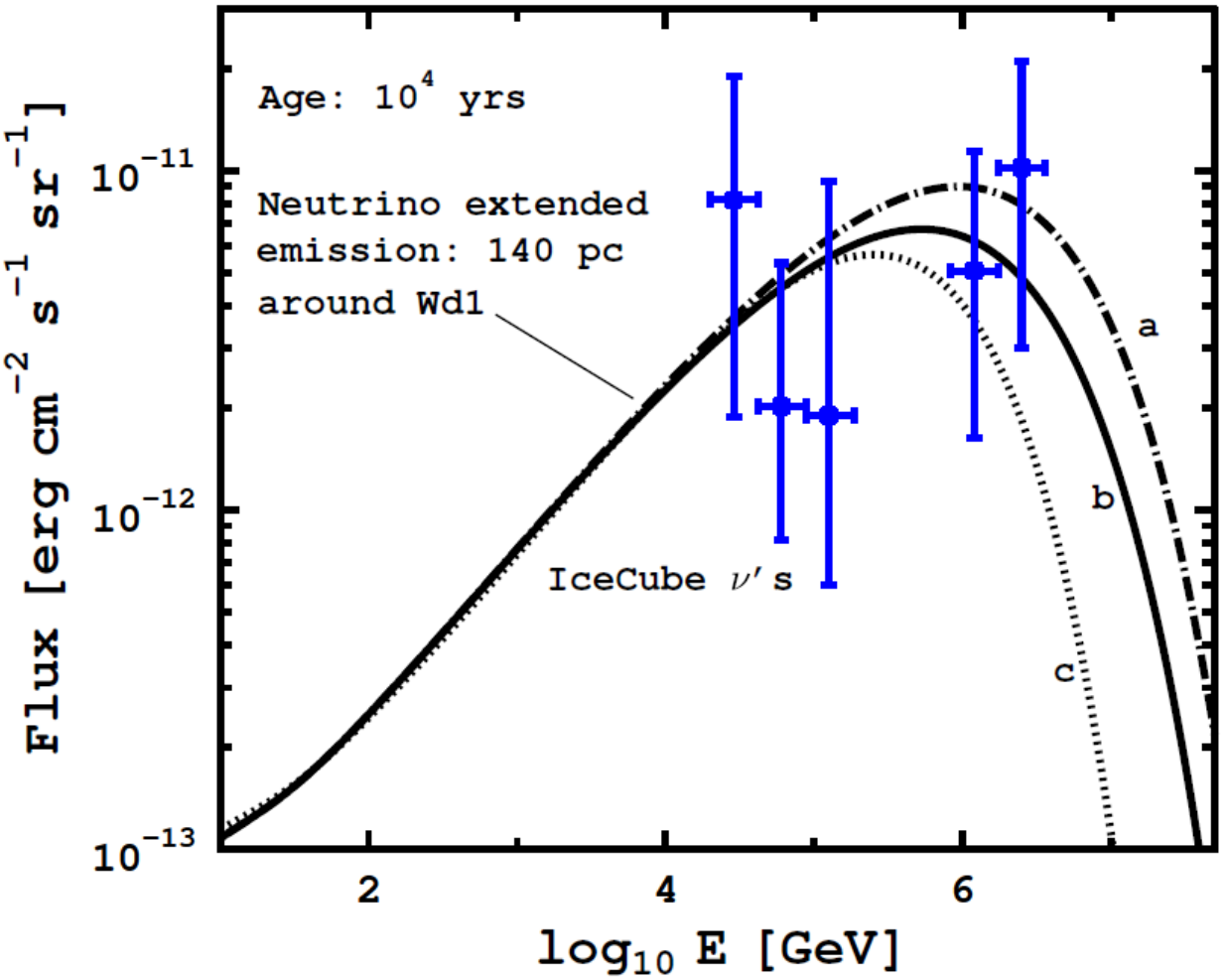

MNRAS V. 453, p. 113, 2015

Secondary pairs synchrotron X-ray counterpart to the Pevatron

A cloud nearby: **SRG perspective?**

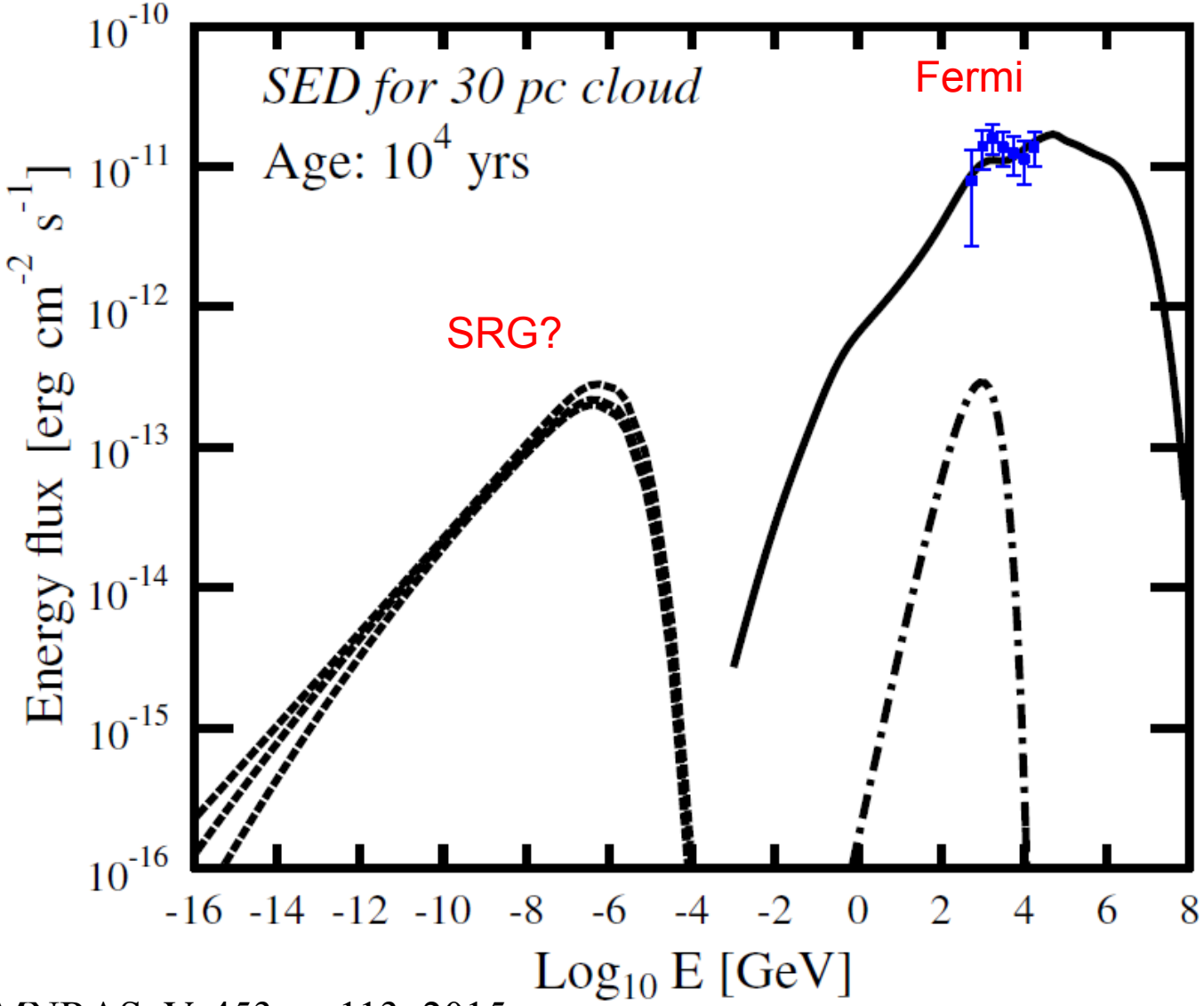

MNRAS V. 453, p. 113, 2015

All Sky Map IceCube 4 years

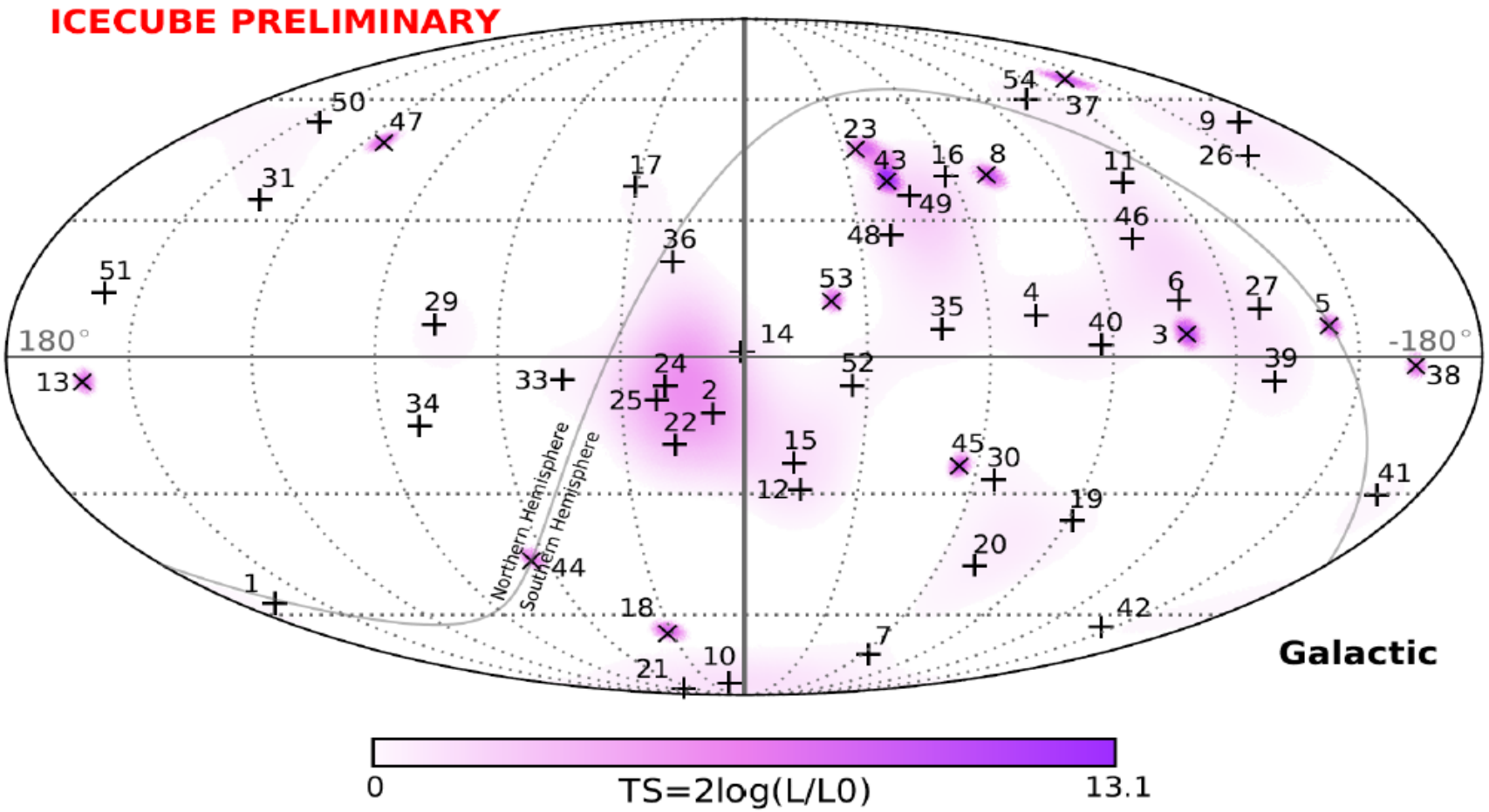

IceCube events in the vicinity of Wd I

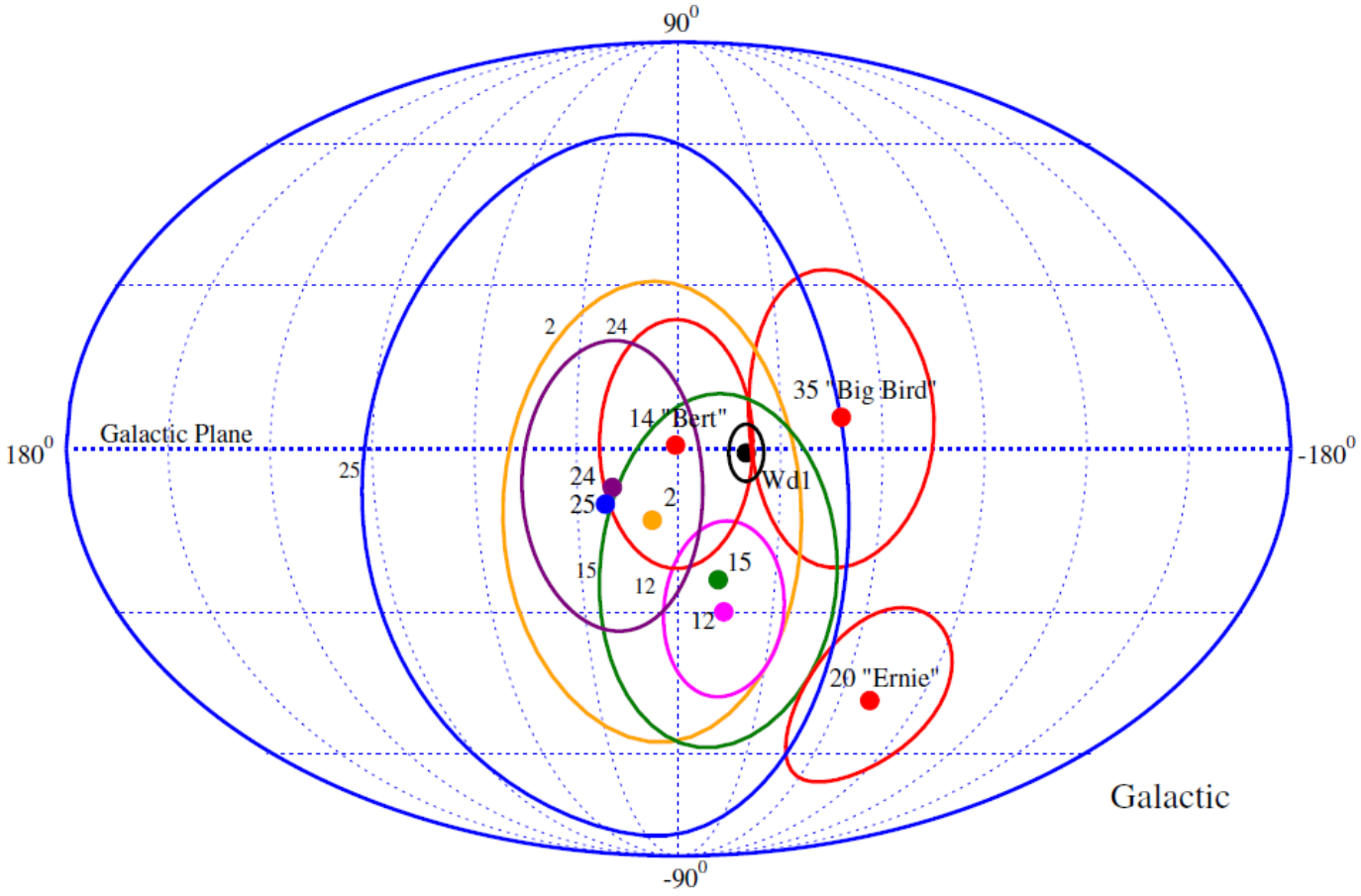

A.B. + 2015

MNRAS V. 453, p. 113, 2015

H.E.S.S. J1808-204

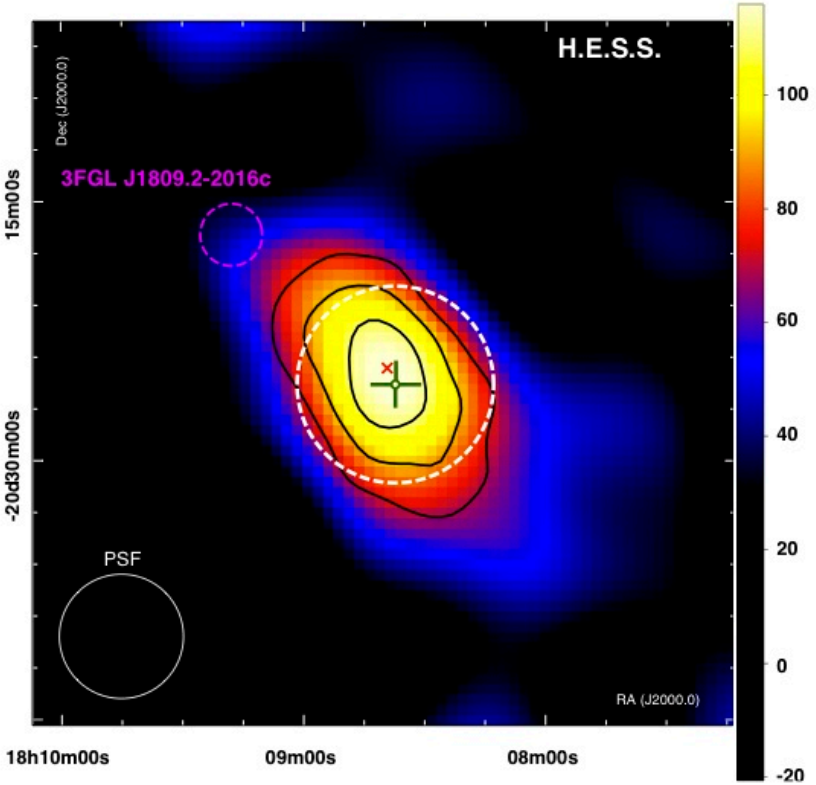

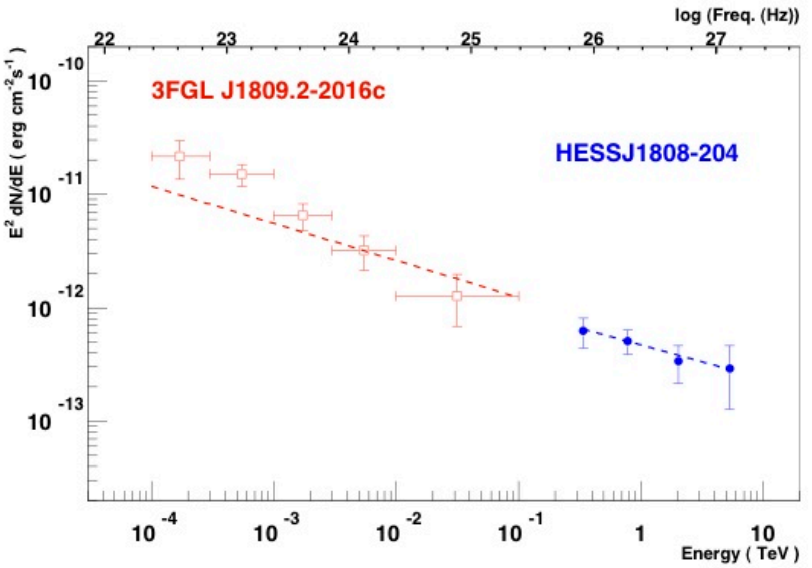

Fig. 2. Energy fluxes, 1 σ statistical errors, and fitted pure power-law fits for HESS J1808−204 (blue solid points and blue dashed line) and the *Fermi-LAT* source 3FGL J1809.2−2016c (red open squares and red dashed line) from Acero et al. (2015).

power-law photon index of 2.3 ± 0.2stat ± 0.3sys
Lvhe ~ 1.6 × 10^(34)[D/8.7 kpc]^2 erg/s

Extended very high-energy gamma-ray source towards the luminous blue variable candidate LBV 1806−20, massive stellar cluster Cl* 1806−20, and magnetar SGR 1806−20 of estimated age about 650 years.

H.E.S.S. collaboration arxiv 1606.05404 2016

3FGL J1809

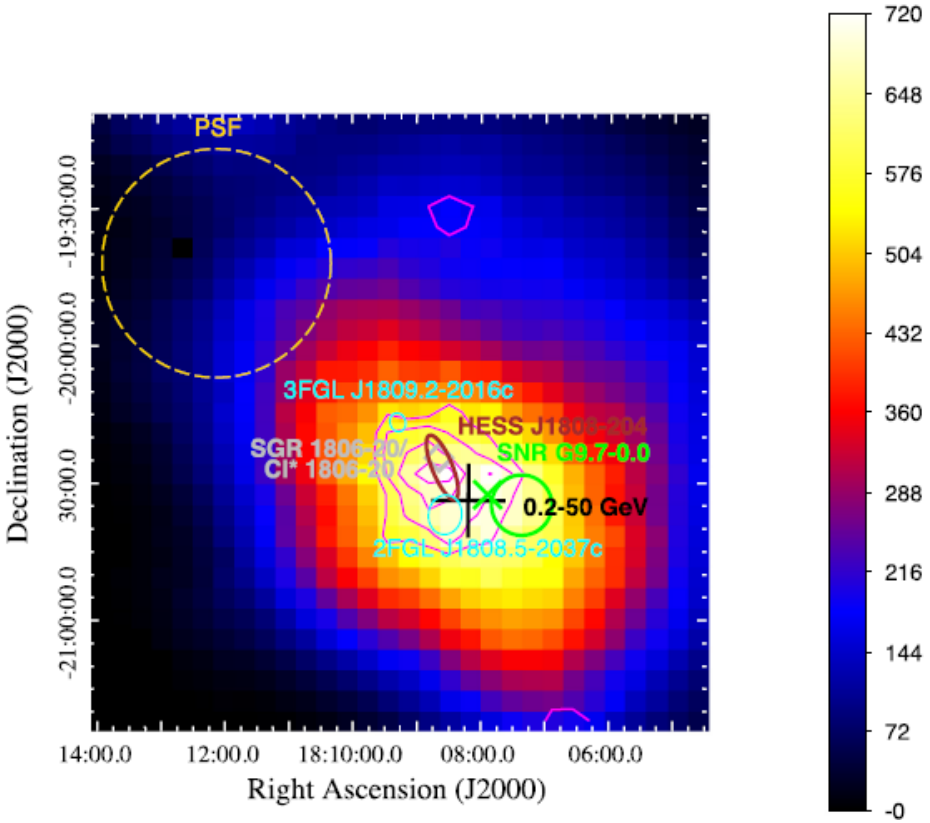

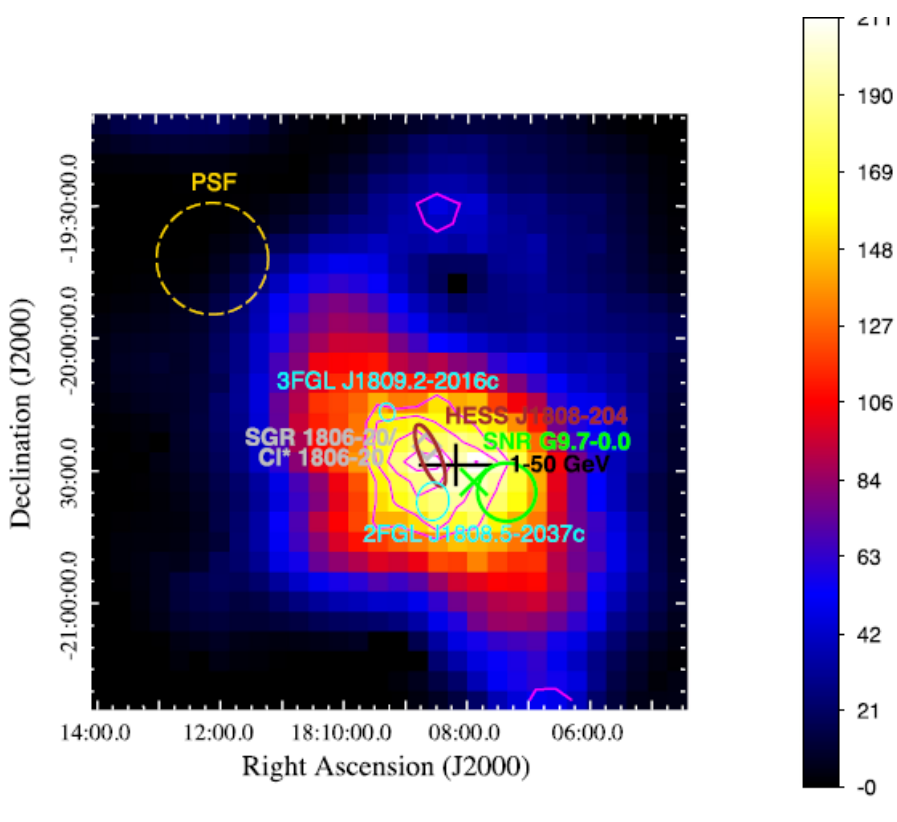

Yeung + 2016

Figure 1. TS maps in 0.2–50 GeV (top) and 1–50 GeV (bottom), respectively, where all neighboring 3FGL catalog sources except 3FGL J1809.2-2016c are subtracted. On each map, the 95% confidence region of the centroid is indicated as a black thick cross, and the FWHM of the PSF is illustrated by a golden dashed circle. Both panels are overlaid with the magenta contours of detection significance (4, 4.5, 5, 5.5σ) determined in 2.5–500 GeV. The position and extents of HESS J1808-204, described as a thick brown ellipse, are taken from Rowell et al. (2012). The position and dimension of SNR G9.7-0.0, described by a green thick circle, are taken from Brogan et al. (2006), and the position of its OH maser, indicated as a green "X", is taken from Hewitt & Yusef-Zadeh (2009). The position of SGR 1806-20/Cl* 1806-20, indicated as a gray diamond, is taken from Israel et al. (2005).

H.E.S.S. J1808-204

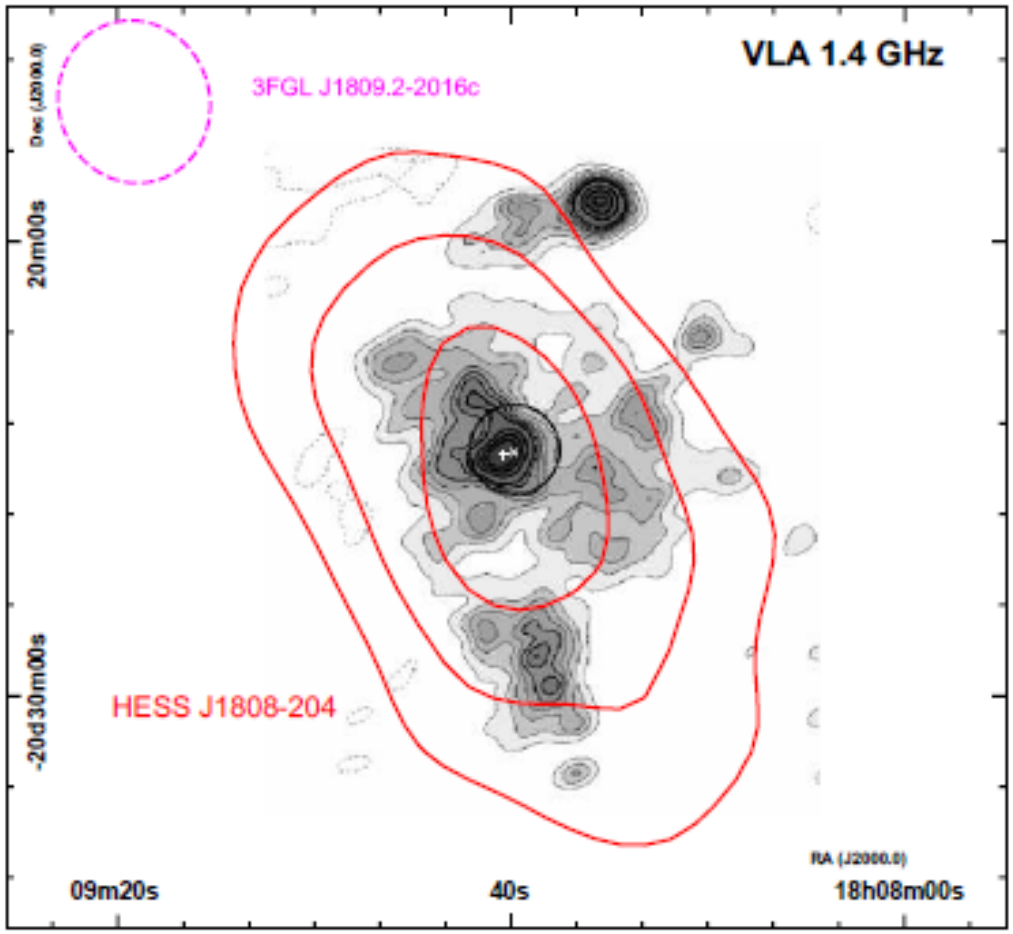

H.E.S.S. J1808-204 model

with gamma-rays from the H.E.S.S. imaged region and total "calorimeter" neutrinos (IC flux is for a few "nearby" events only)

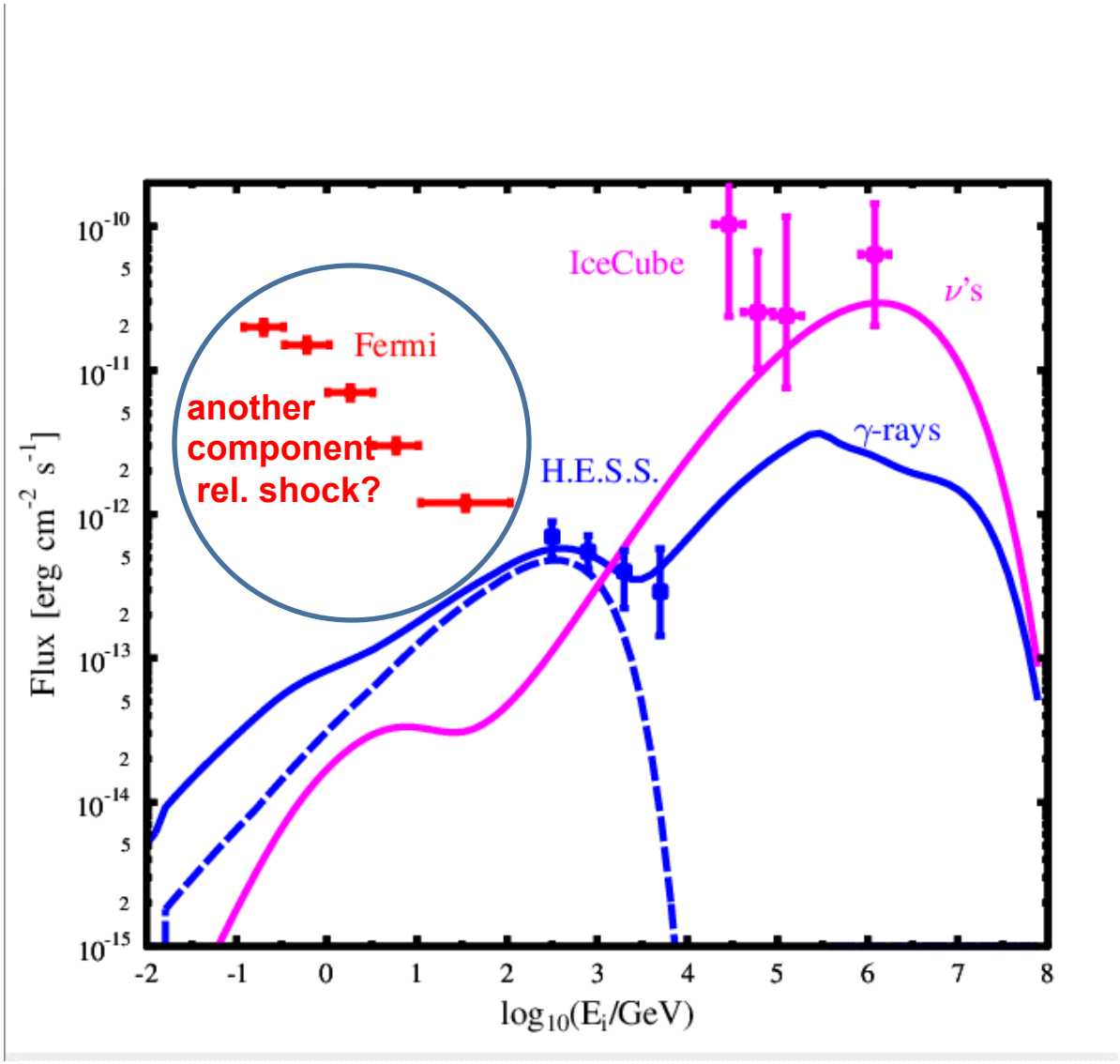

H.E.S.S. J1808-204 model
total "calorimeter" gamma-rays

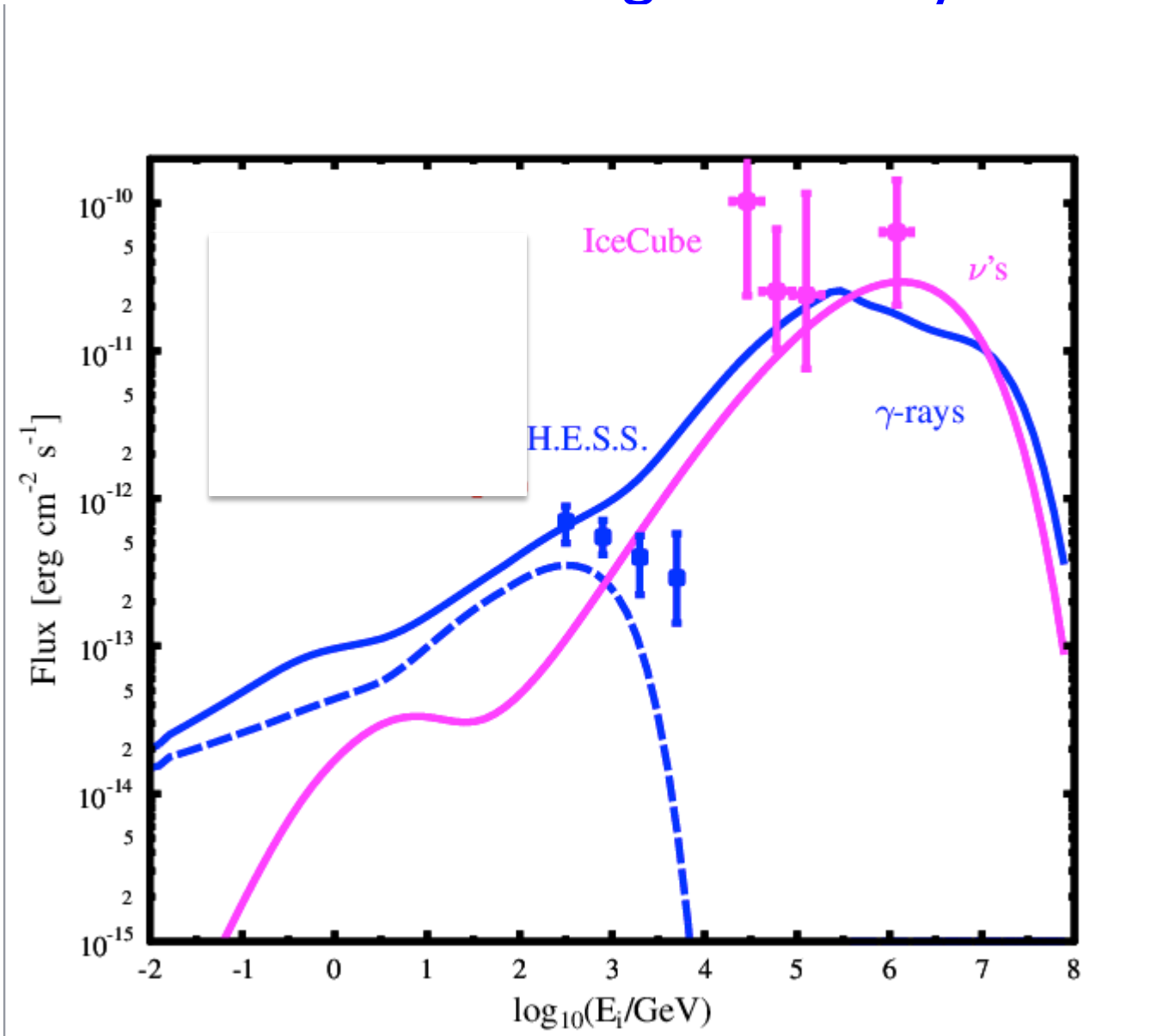

Potential IceCube events from galactic SNe in young star clusters

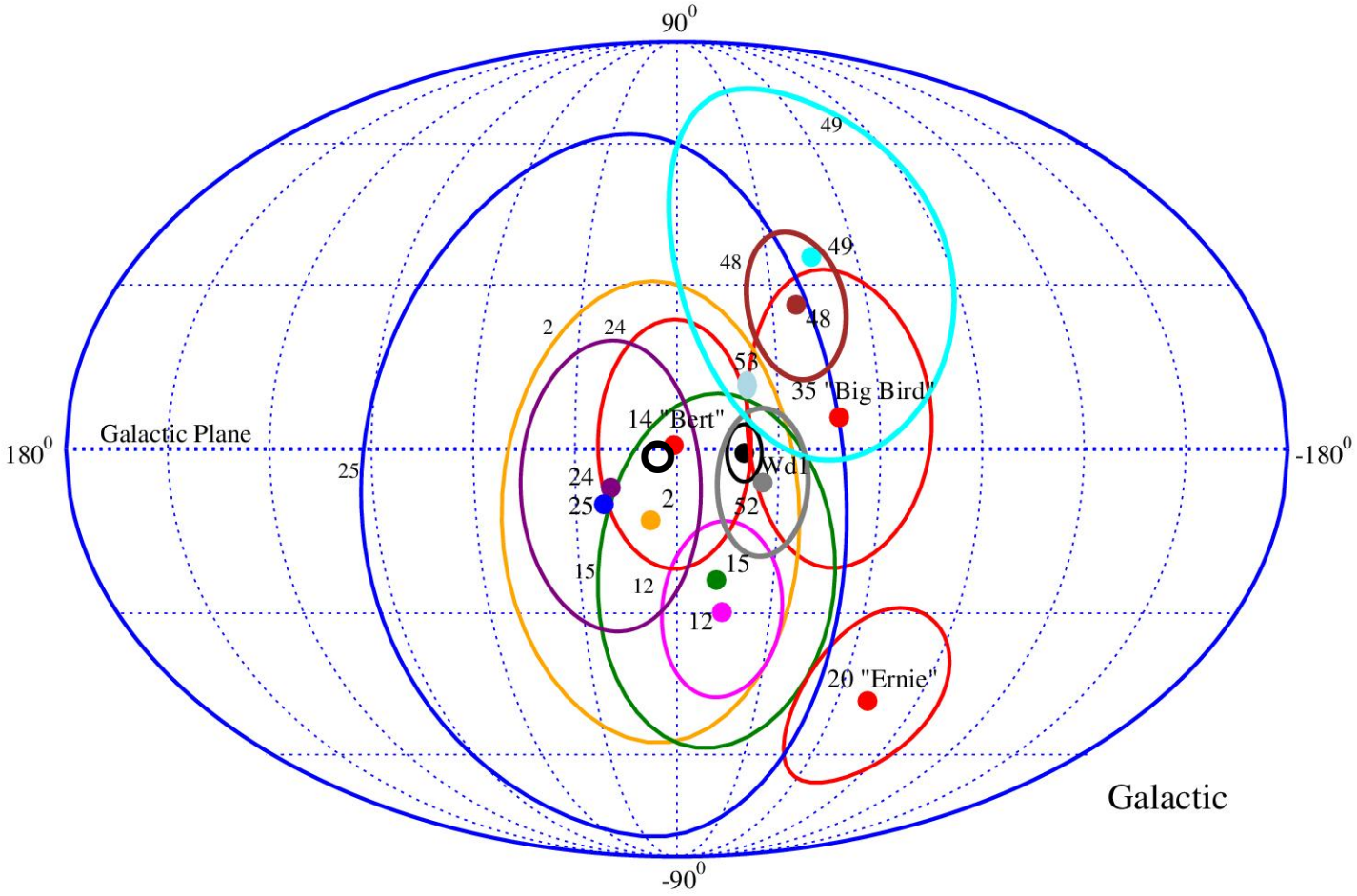

Wd l = 339 32 57.6; b = -00 24 15.0 (black filled circle)
SGR1806 l=09 58 42.0; b=-00 14 33.3 (black open circle)

Currently the expected amount of PeV sources like SNe – cluster wind collision in the Milky Way is likely a few

However, the sources are likely dominated in the starburst galaxies (hundreds of clusters) with the high ISM pressure due to mergers etc.

They may be the CR sources for the Waxman-Bahcall starburst calorimeter hypothesis

Waxman-Bahcall prediction

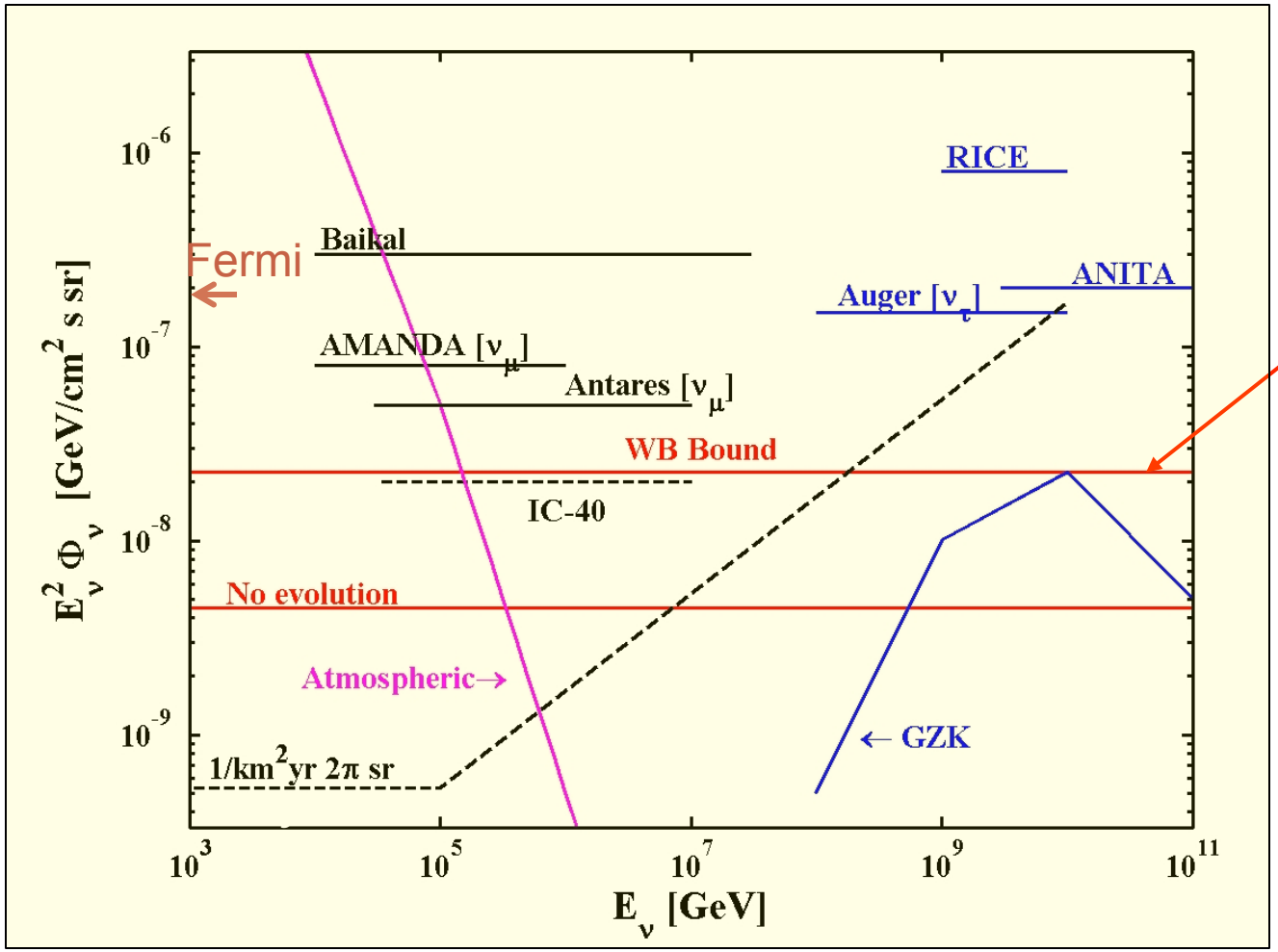

$$\frac{E^2 d\dot{n}/dE}{10^{44}\,\mathrm{erg/Mpc^3 yr}} = 0.5$$

Starburst “calorimeter” model

Core-collapse - SN rate

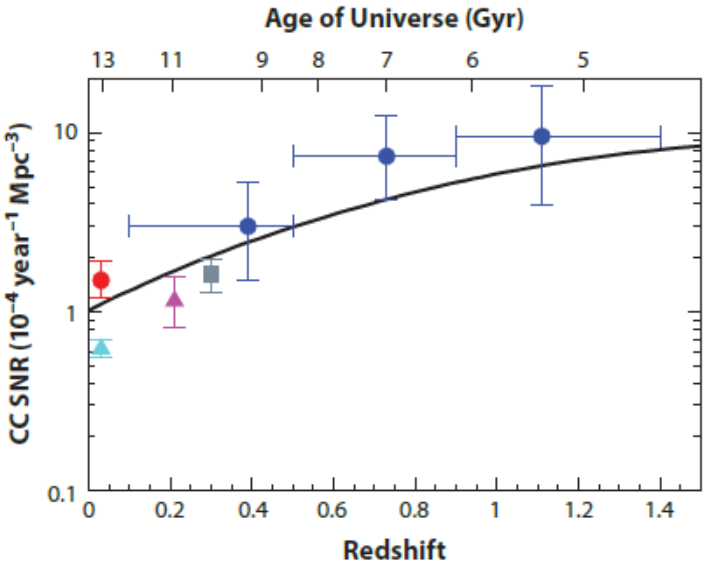

Figure 10

The cosmic core-collapse supernova (SN) rate. The data points are taken from Li et al. (2011) (*cyan triangle*), Mattila et al. (2012) (*red dot*), Botticella et al. (2008) (*magenta triangle*), Bazin et al. (2009) (*gray square*), and Dahlen et al. (2012) (*blue dots*). The solid line shows the rates predicted from our fit to the cosmic star-formation history. The local overdensity in star formation may boost the local rate within 10–15 Mpc of Mattila et al. (2012).

$$R_{\rm CC}(z) = \psi(z) \times \frac{\int_{m_{\rm min}}^{m_{\rm max}} \phi(m){\rm d}m}{\int_{m_l}^{m_u} m\phi(m){\rm d}m} \equiv \psi(z) \times k_{\rm CC}, \qquad (16)$$

where the number of stars that explode as SNe per unit mass is $k_{\rm CC} = 0.0068\ {\rm M}_\odot^{-1}$ for a Salpeter IMF, $m_{\rm min} = 8\,{\rm M}_\odot$ and $m_{\rm max} = 40\,{\rm M}_\odot$. The predicted cosmic SN rate is shown in **Figure 10**

Madau & Dickinson, ARAA 2014

Cluster formation efficiency

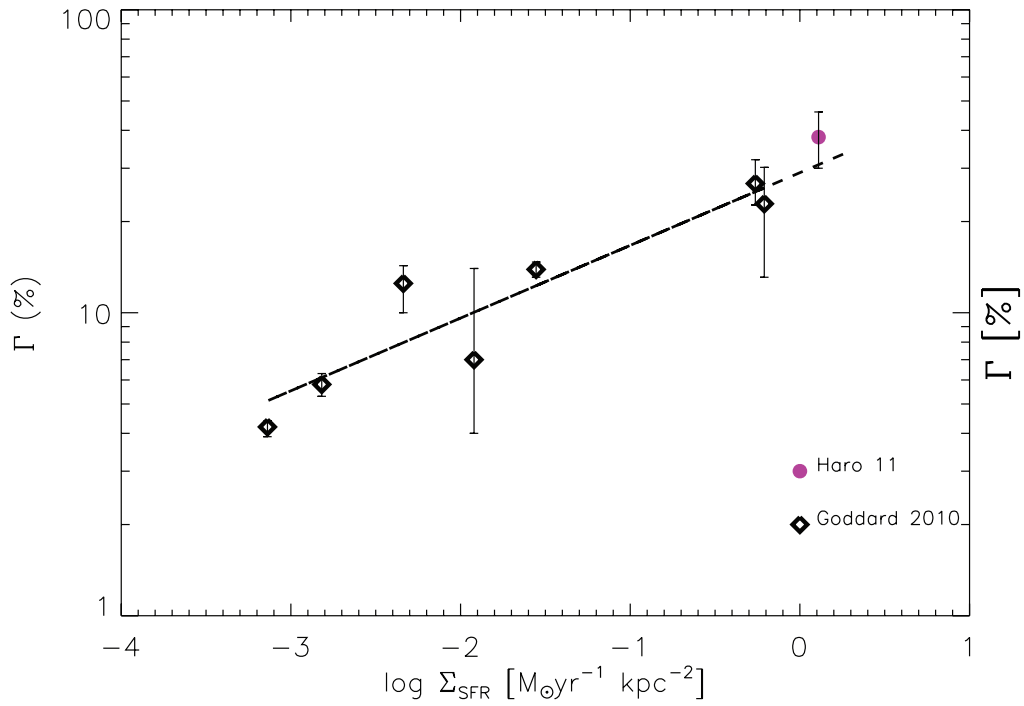

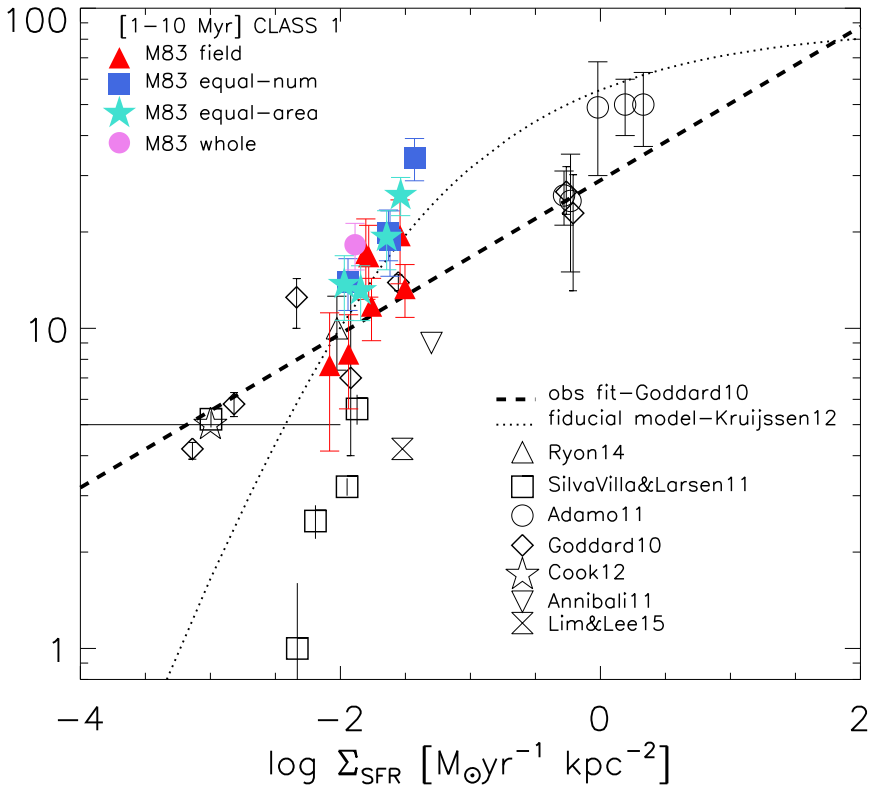

Figure 23. Cluster formation efficiency, Γ, as a function of the galactic SFR density, Σ_{SFR}. The black diamonds are the galaxy sample of Goddard et al. (2010) which were used to obtain the best-fitting power-low relation shown by the dashed line (Goddard et al. 2010, their equation 3). At the right-hand end we show the position of Haro 11 (filled dots) which fits the relation nicely despite its extreme Γ and SFR values.

SFR in Haro 11 galaxy is about 22 Msun/yr

Adamo + 2010

Adamo & Bastian 2016

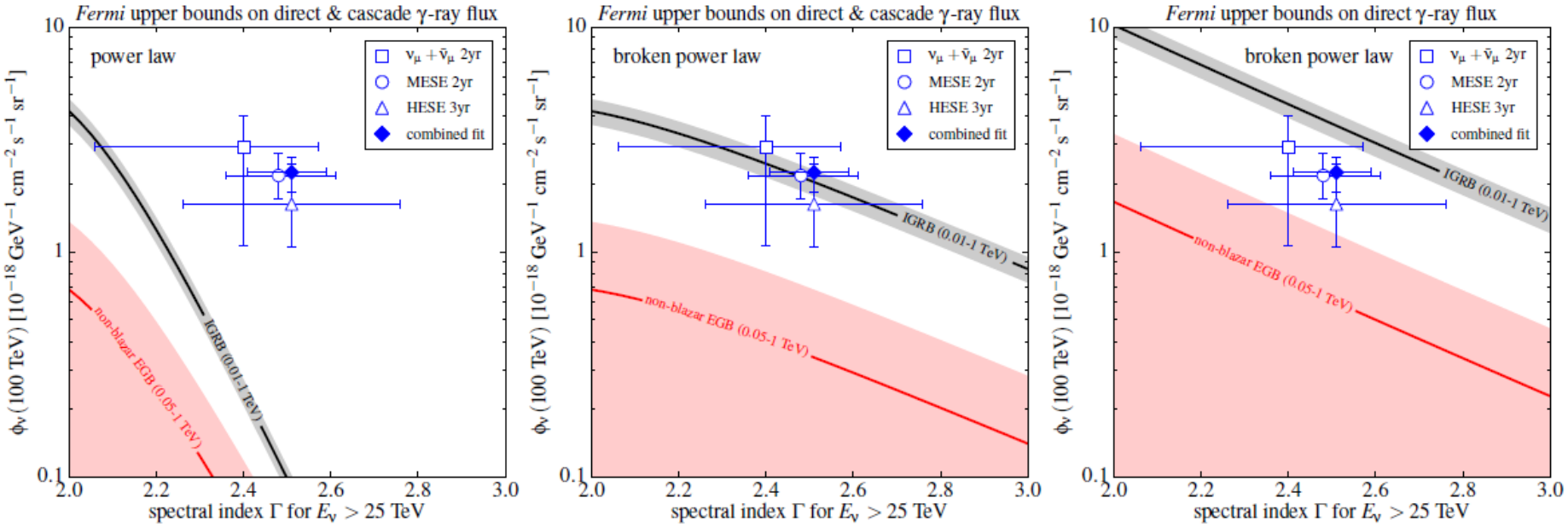

FIG. 2. Upper limits on the per-flavor normalization $\phi_\nu(100\text{TeV})$ of the isotropic neutrino flux depending on the spectral index Γ for $E_\nu \gtrsim 25$ TeV. The black and red lines show the upper limits from the IGRB (0.01–1 TeV) and from the non-blazar EGB (0.05–1 TeV), respectively. Both results are shown with uncertainty bands. The left panel shows the constraints for a simple power-law emission spectrum. The center and right panel show the results for a broken power-law model following Eq. (1). For illustration, we show the results separately for the total (direct + electromagnetic cascade) γ-ray emission (center panel) and only the direct γ-ray emission (right panel). The data points show the best-fit power-law neutrino spectrum including the 68% C.L. range in terms of the spectral index Γ and astrophysical normalization at 100 TeV estimated by IceCube analysis: the high-energy starting event (HESE) analysis [45], the medium-energy starting event (MESE) analysis [46] and the classical search for up-going $\nu_\mu + \bar{\nu}_\mu$ tracks [47]. The values are extracted from Ref. [1], which also derives a global fit to the data.

K.Bechtol, M. Ahlers, M. Di Mauro,. M. Ajello, J. Vandenbroucke 2015

SNe in YMSCs can accelerate CRs well above PeV with a specific hard spectrum of an upturn-type

The efficiency of YMSC formation in starbursts may be ~ 0.4

Then ~ 10^{-5} Mpc^{-3} yr^{-1} of CC SNe are YMSCs in starbursts providing CR power > 10^{44} ergs Mpc^{-3} yr^{-1}

This is consistent with the Waxman-Bahcall starburst calorimeter and the hard spectrum allows to avoid a conflict with Fermi gamma-ray diffuse emission flux

Acceleration of petaelectronvolt protons in the Galactic Centre?

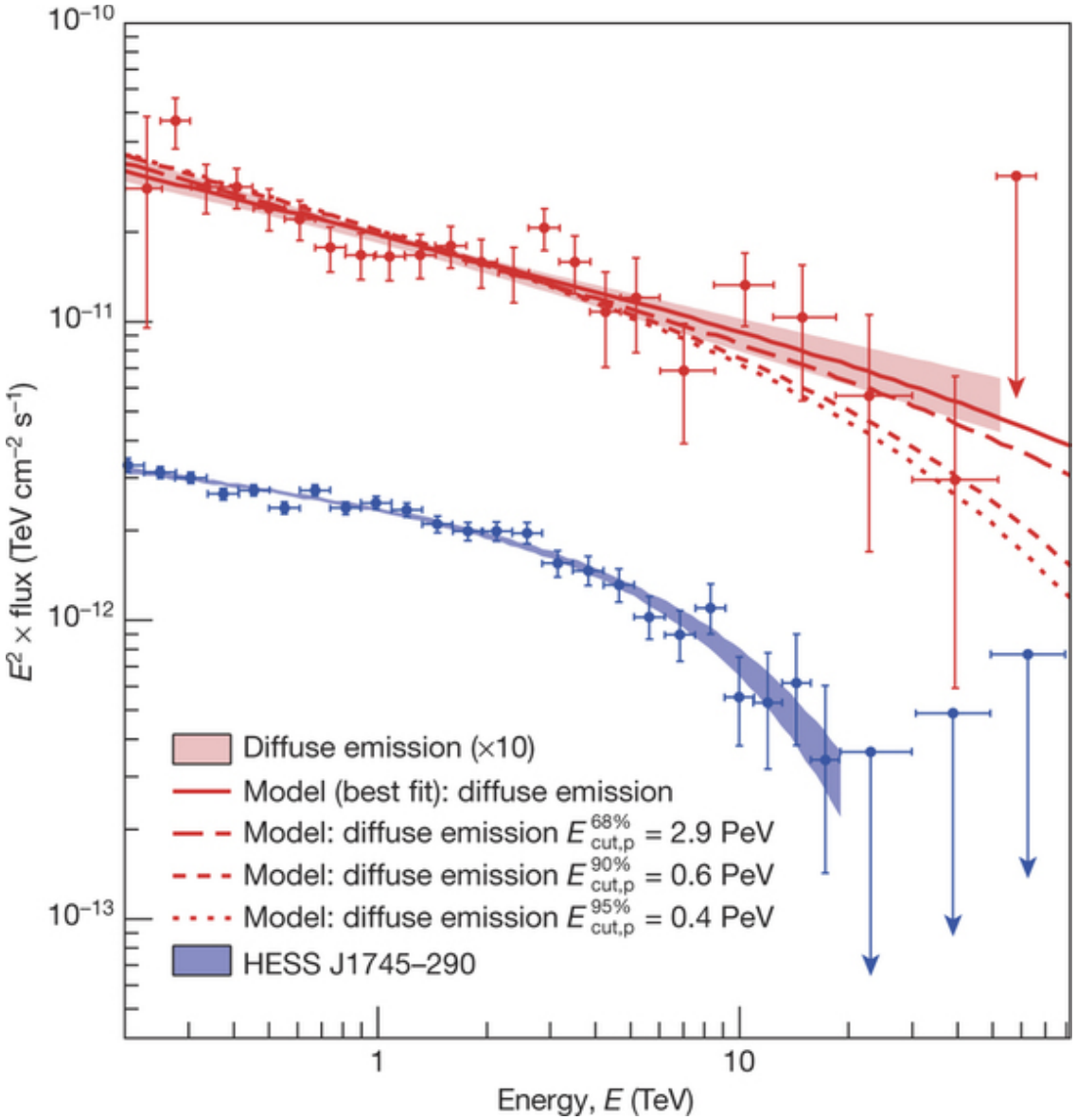

SNR in GC wind?
YMSC wind- Sne?

HESS collaboration Nature 531, 476, 2016

Thanks for your attention!

Acknowledge support from RSF grant 16-12-10225

Monte Carlo modeling of DSA Magnetic Field Amplification

Conservation laws in MC modeling

$$\rho(x)u(x) = \rho_0 u_0 \quad \text{- mass}$$

$$\rho(x)u^2(x) + P_{th}(x) + P_{cr}(x) + P_w(x) = \Phi_{P0} \quad \text{- momentum}$$

$$\frac{\rho(x)u^3(x)}{2} + F_{th}(x) + F_{cr}(x) + F_w(x) + Q_{esc} = \Phi_{E0} \quad \text{- energy}$$

Energy flux background plasma

$$F_{th}(x) = u(x)\frac{\gamma_g P_{th}(x)}{\gamma_g - 1}$$

Energy flux and turbulent pressure

$$F_w(x,k) = \frac{3}{2}u(x)W(x,k) \qquad P_w(x,k) = \frac{W(x,k)}{2}$$

Magnetic Fluctuation Spectral Evolution

$$\frac{\partial F_w(x,k)}{\partial x} + \frac{\partial \Pi(x,k)}{\partial x} = u(x)\frac{\partial P_w(x,k)}{\partial x} + \Gamma(x,k)W(x,k) - L(x,k)$$

Energy flux components

$$\frac{dF_w(x)}{dx} = u(x)\frac{dP_w(x)}{dx} + \int_{(k)} \Gamma(x,k)W(x,k)dk - L(x)$$

$$\frac{dF_{th}(x)}{dx} = u(x)\frac{dP_{th}(x)}{dx} + L(x)$$

$$\frac{dF_{cr}(x)}{dx} = \left[u(x) + v_{scat}(x)\right]\frac{dP_{cr}}{dx}$$

$$v_{scat}(x) = -\int_{(k)} \Gamma(x,k)W(x,k)dk \Big/ \frac{dP_{cr}}{dx}$$

AB +., ApJ, 789:137, 2014.

Bulk velocity and magnetic field profiles

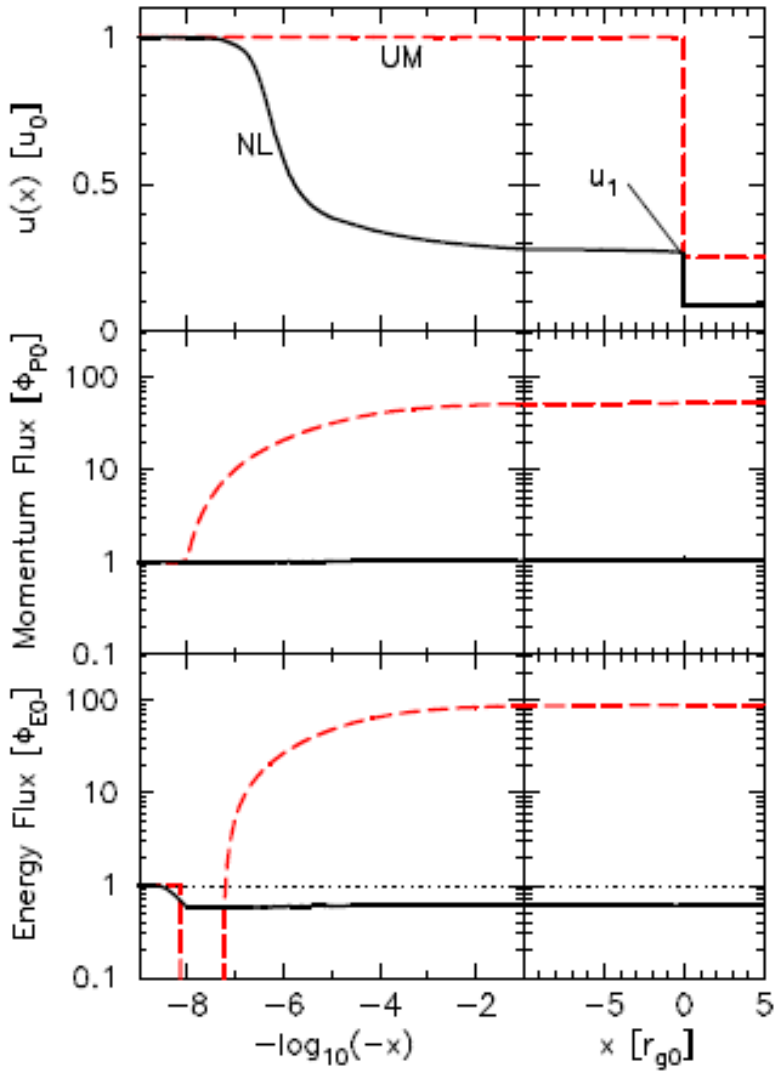

$$r_{g0} = \frac{m_p c u_0}{eB_0}$$

$n_0 = 0.3\ см^{-3};\ u_0 = 5000\ \frac{км}{с};\ B_0 = 3$ мкГс

AB +., ApJ, 789:137, 2014.

Magnetic turbulence spectra

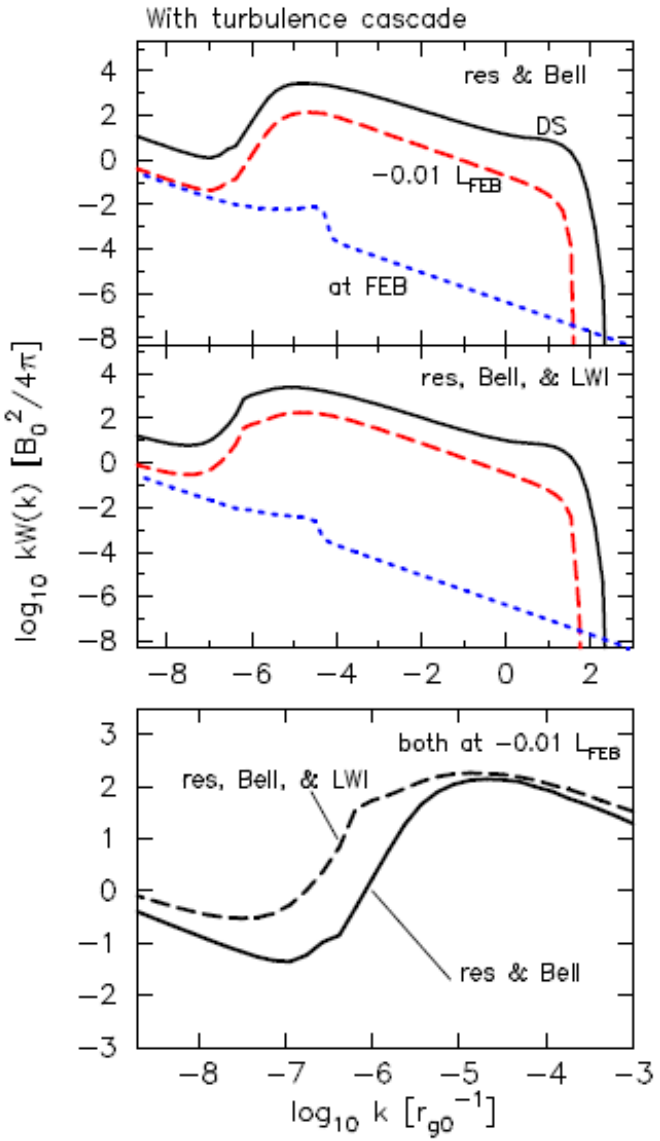

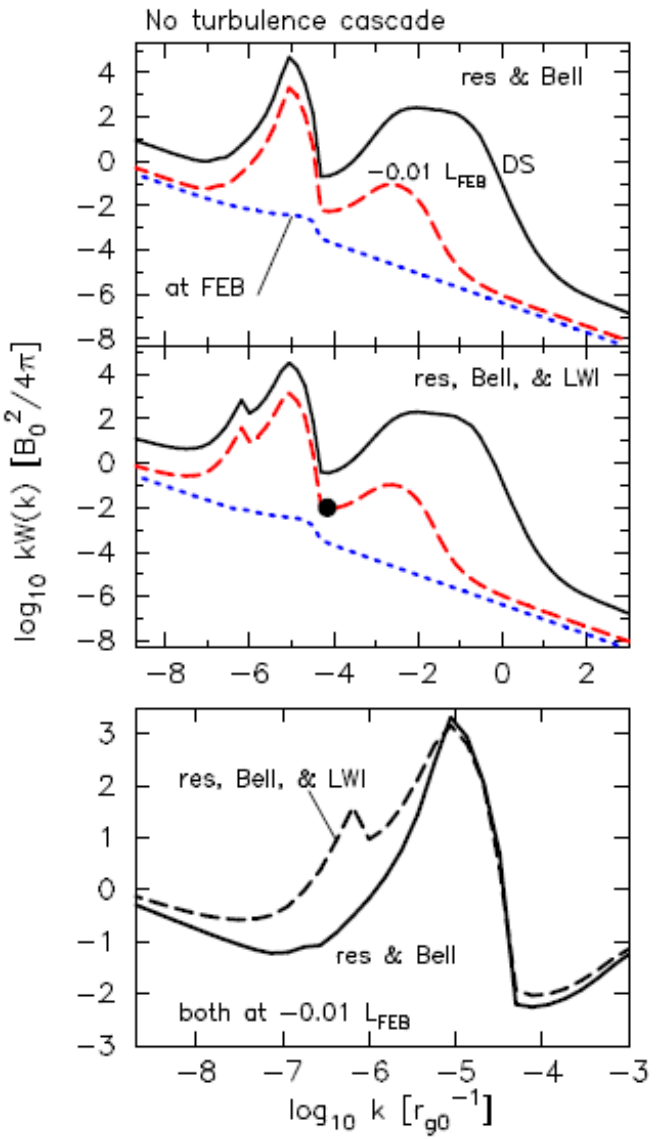

$$n_0 = 0.3\ см^{-3};\ u_0 = 5000\ \frac{км}{с};\ B_0 = 3\ мкГс$$

ApJ, 789:137, 2014.

Fluctuating magnetic field and magnetic pressure scalings

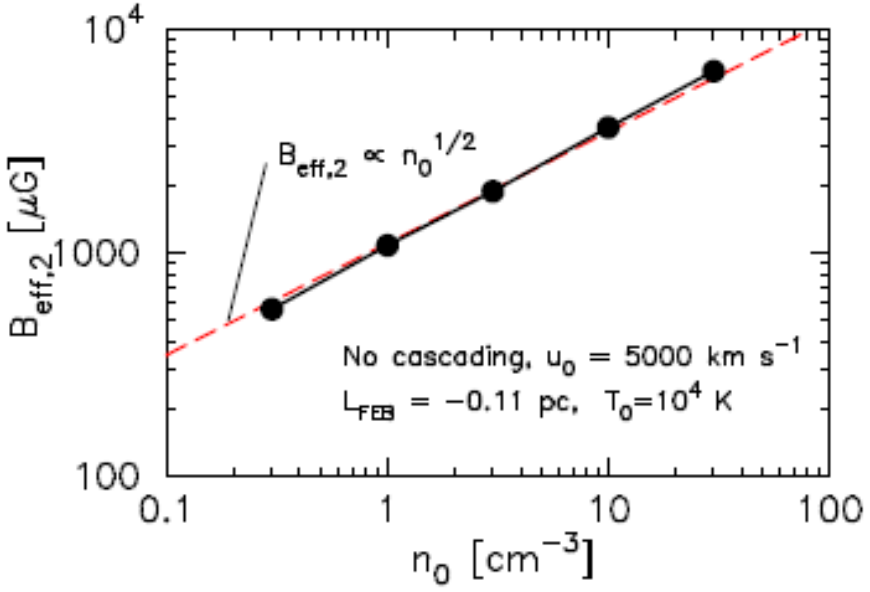

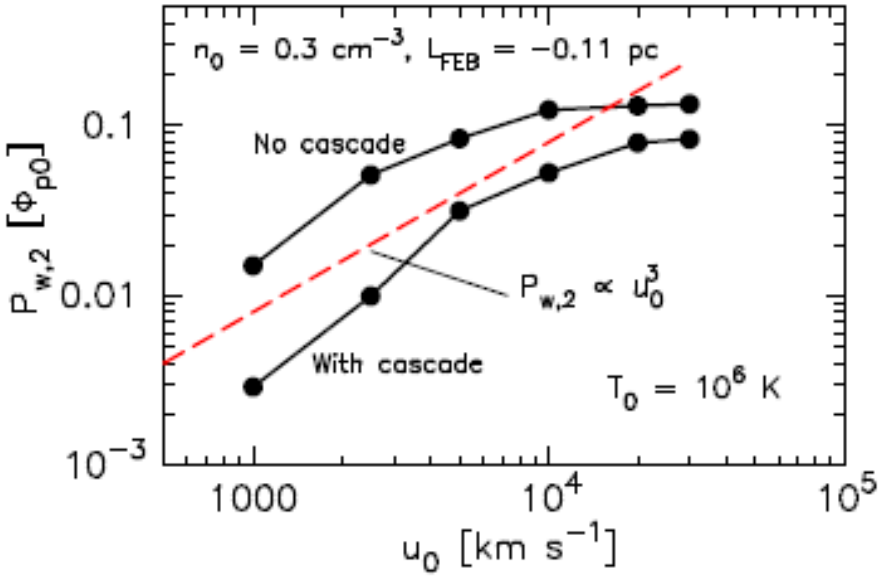

$$B_{eff,2} \propto \sqrt{n_0 u_0^{\theta}}$$

$$\frac{B_{eff,2}^2}{n_0} \propto u_0^3 \rightarrow \theta : 1.5$$

, **ApJ, 789:137, 2014.**

CR spectra scalings

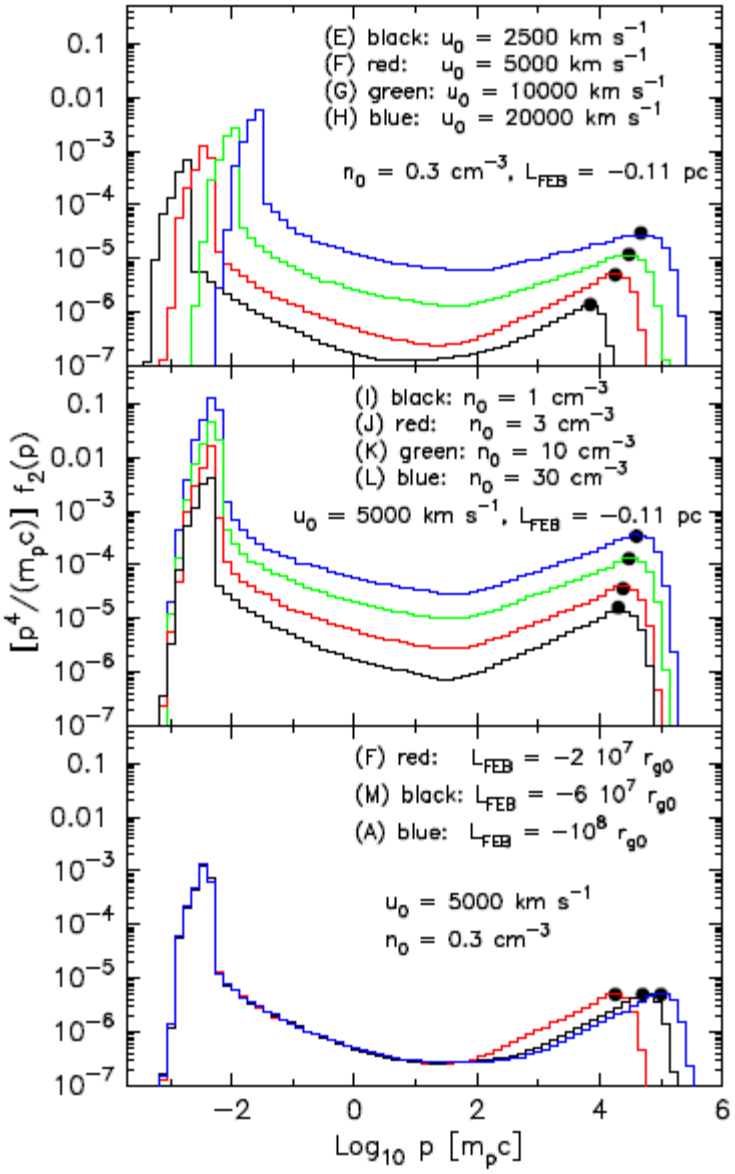

Maximal momentum of accelerated CRs

$$p_{\max} \propto n_0^{\delta} u_0 L_{FEB}$$

δ : 0.25

ApJ, 789:137, 2014.

Scattering center velocity vs Alfven speed

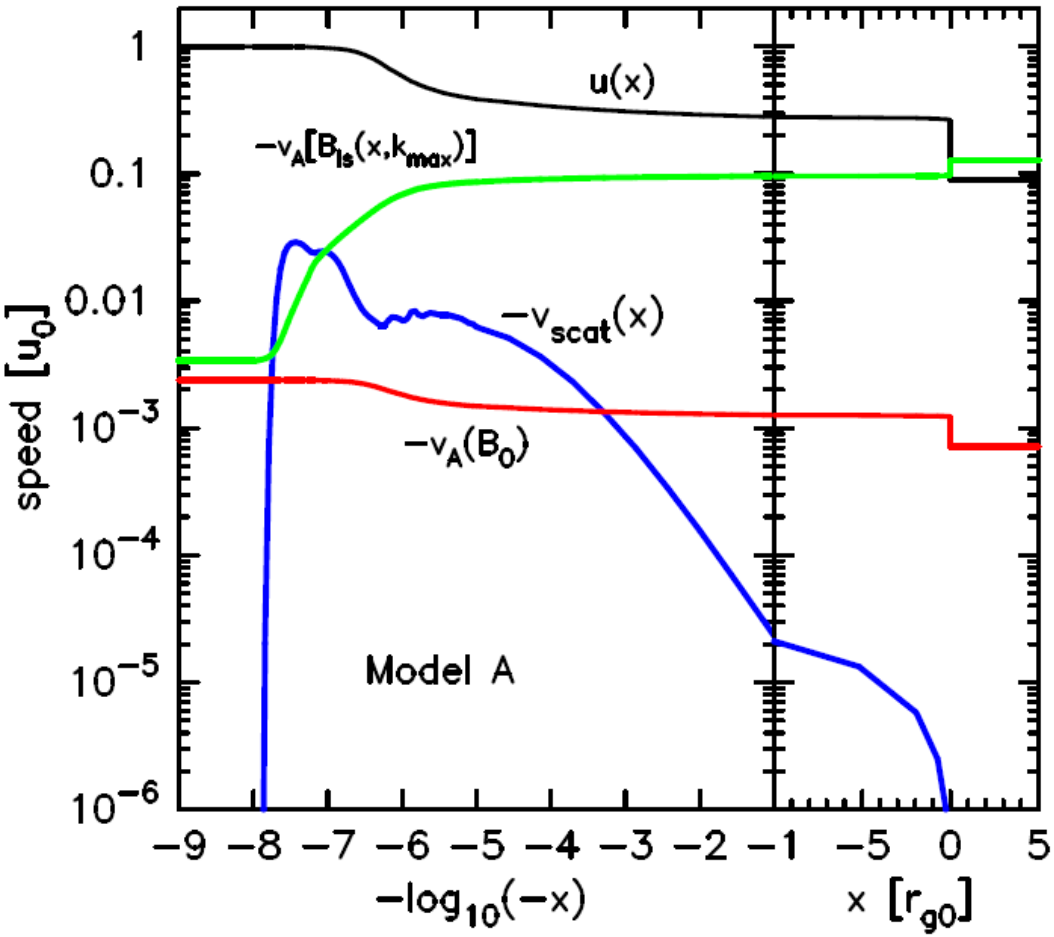

$$n_0 = 0.3\ см^{-3};\ u_0 = 5000\ \frac{км}{с};\ B_0 = 3\ мкГс$$

ApJ, 789:137, 2014.

IceCube neutrinos galactic latitude profile > 100 TeV

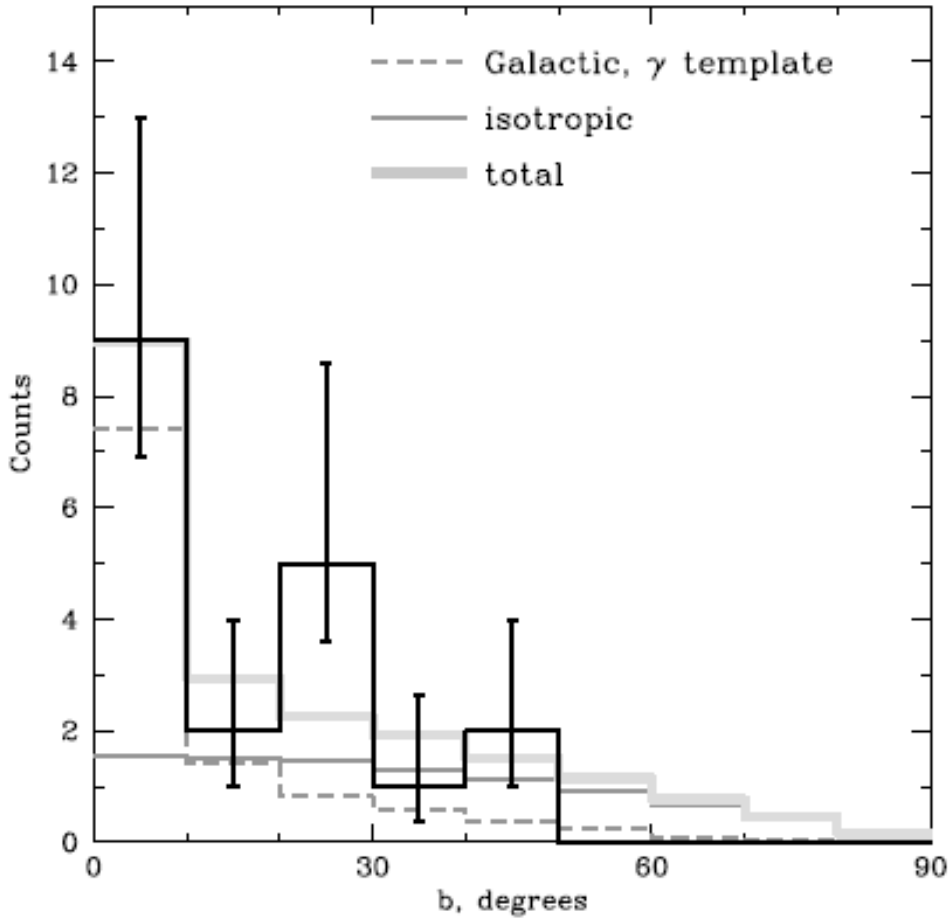

Evidence for the Galactic contribution to the IceCube astrophysical neutrino flux

Neronov & Semikoz Astroparticle Physics, Volume 75, p. 60-63, 2016

Energy conservation in 1D NL colliding shocks model

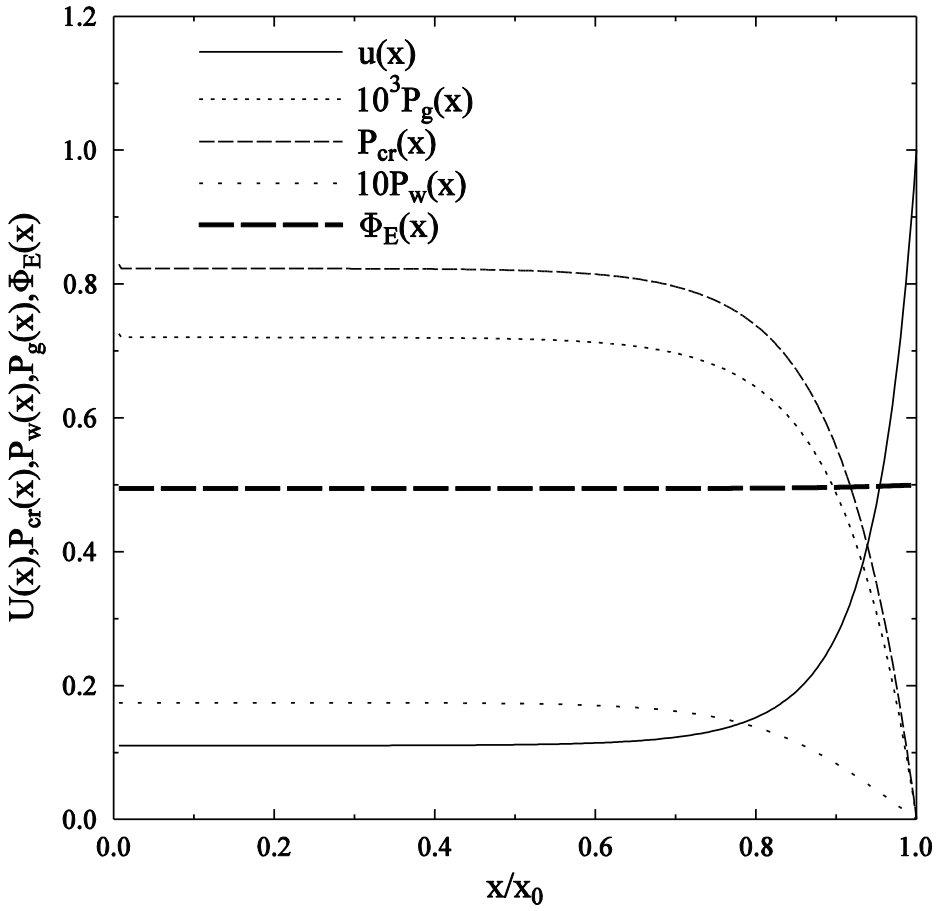

Nonlinear model of LECR spectra in superbubble

MHD Shock-Turbulence Power Conversion to CRs

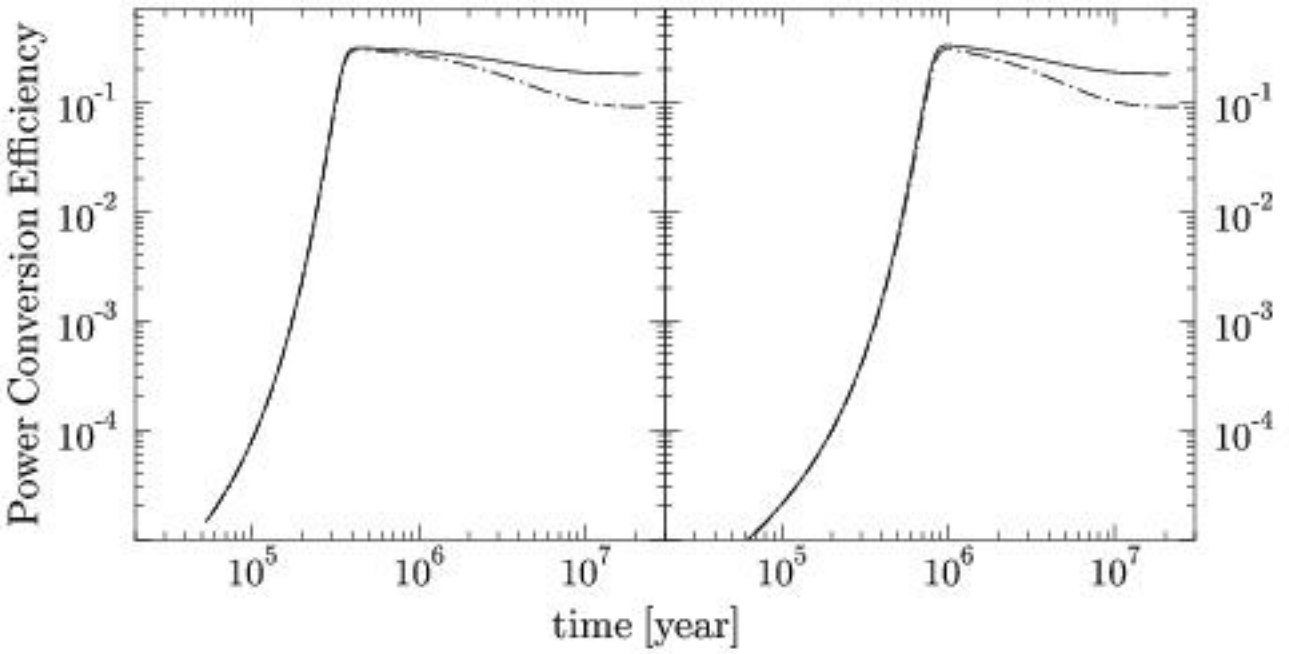

Space Sci. Rev. v.99, 317, 2001; Astron. Astroph. Reviews v22, id 77, 2014

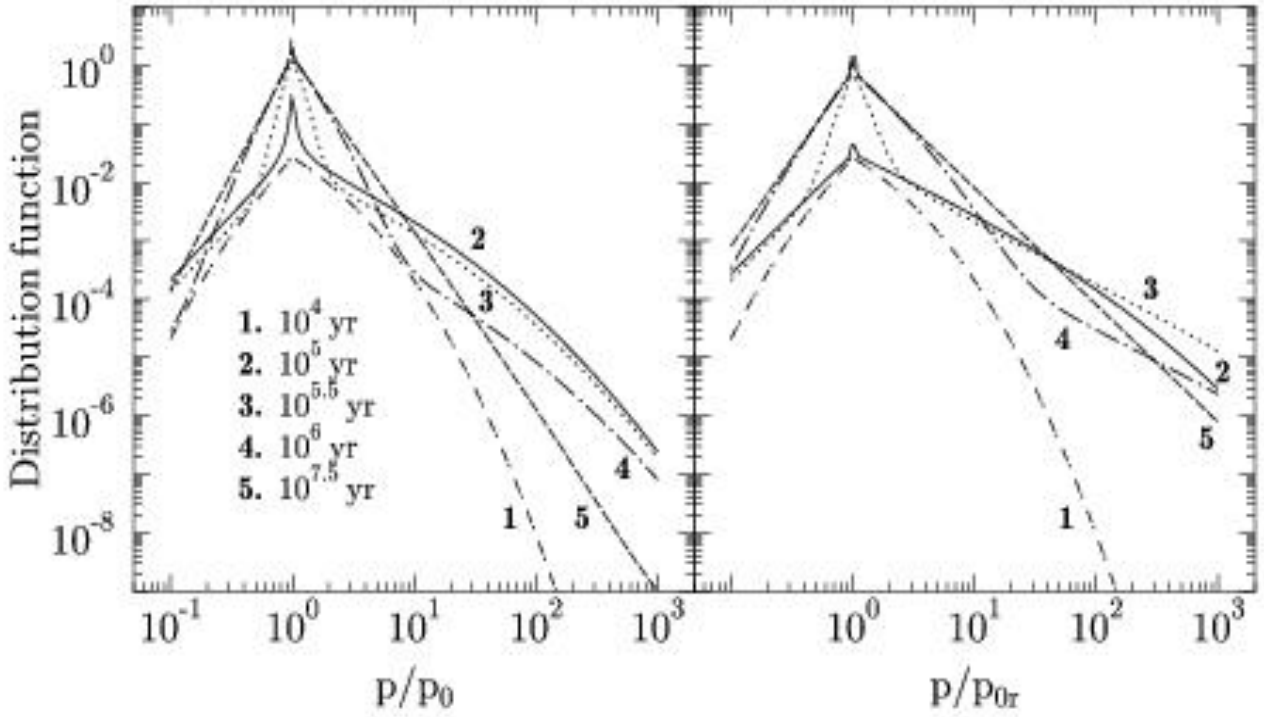

Space Sci. Rev. v.99, 317

Long-time LECR spectra evolution in SB

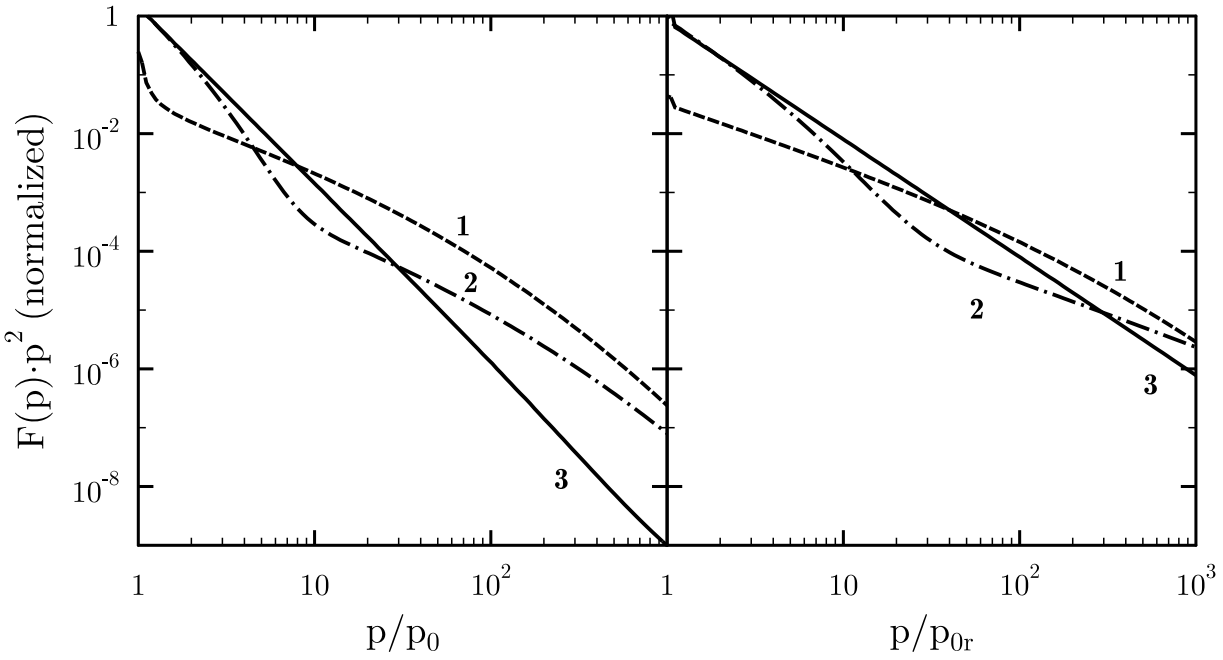

A&ARv v.22, 77, 2014